https://doi.org/10.5194/egusphere-2024-3926
Preprint. Discussion started: 3 February 2025

Evaluating urban methane emissions and their attributes in a megacity, Osaka, Japan, via mobile and eddy covariance measurements

Masahito Ueyama[1], Taku Umezawa[2], Yukio Terao[2], Mark Lunt[3], James Lawrence France[3,4]

[1]Graduate School of Agriculture, Osaka Metropolitan University, Sakai, 599-8531, Japan
[2]National Institute for Environmental Studies, Tsukuba, Ibaraki 305-8506, Japan
[3]Environmental Defense Fund, New York, NY 10010, USA
[4]Earth Sciences Dept, Royal Holloway University of London, TW20 0EQ, Egham, UK

Correspondence to: Masahito Ueyama (mueyama@omu.ac.jp)

Abstract. Urban areas are regions where we expect large amounts of greenhouse gas emissions, but in many urban areas, the sources and sinks have yet to be characterized with certainty. In this study, we conducted mobile and eddy covariance measurements to evaluate CH_4 emissions in the megacity Osaka, Japan. Based on the mobile measurements, several elevated CH_4 concentrations were observed. Most of the locations were not related to CH_4 sources identified by emission inventories reported by local governments. Two platforms for mobile measurements, vehicle and bicycle, showed good consistency for estimating total CH_4 emissions, but vehicle measurements tended to result in smaller natural gas emission estimates than bicycle measurements did. The estimated CH_4 emissions were 10,021 ± 1,000 tCH_4 yr^{-1} for Osaka city and 2,379 ± 480 tCH_4 yr^{-1} for Sakai city, 18 times and 2.5 times greater, respectively, than those expected in the inventories. Coincident C_2H_6 observations indicated that natural gas emissions contributed 64% of the total CH_4 emissions in Osaka city and 47% in Sakai city. The upscaled CH_4 emissions were calibrated with the daytime CH_4 fluxes via the eddy covariance method, as the empirical models significantly underestimated the regional fluxes. From these snapshots, the CH_4 emissions from the metropolitan areas in Japan may be considerably greater than the emission inventories, and most CH_4 sources are not well characterized in those inventories. These unaccounted sources need to be better characterized to improve the Japanese CH_4 inventory and assess whether these emissions can be mitigated.

1 Introduction

Cities are among the major sources of greenhouse gases and are thus important targets for emission reduction (e.g., Crippa et al. 2021). In particular, methane (CH_4) emission reduction is important in the medium term because CH_4 is a powerful greenhouse gas whose global warming potential is 84 times greater than that of carbon dioxide (CO_2) for a 20-year time horizon. Consequently, there is an urgent need to reduce CH_4 emissions for a short-term positive effect on climate warming. Recent measurements of CH_4 concentrations and fluxes in urban areas suggest that substantial CH_4 emissions occur in many cities and that emission inventories are highly uncertain, especially in terms of urban natural gas emissions (Helfter et al.,

https://doi.org/10.5194/egusphere-2024-3926
Preprint. Discussion started: 3 February 2025

2016; Sargent et al. 2021). More independent assessments of emission inventories for different cities are needed to drive effective mitigation actions.

In recent years, measurements using vehicle-mounted instruments have been carried out in urban areas to compare CH_4 emissions among different urban environments. These studies highlighted that 1) urban regions are significant CH_4 sources (Vogel et al., 2024), 2) some CH_4 sources do not account for the current inventories (Vogel et al., 2024), 3) nonnegligible levels of gas leaks from sewer networks (Fernandez et al., 2022; Joo et al., 2024) or underground gas pipelines, mostly old corrosion-prone pipelines (Defratyka et al., 2021; von Fischer et al., 2017), and 4) a small number of high CH_4 emission rates mostly account for an area's total CH_4 emissions (Maazallahi et al., 2020). Previous studies have also revealed large varieties of emission characteristics in terms of emission intensity and attributions. Currently, most of these measurements have been conducted in Europe and North America (e.g., Vogel et al., 2024), and most Asian megacities, except Seoul, South Korea (Joo et al., 2024), are underrepresented.

Ethane (C_2H_6) is a useful tracer for estimating leakage from natural gas distribution systems, as natural gas has a characteristic CH_4 to C_2H_6 ratio. Gas leakage was recently estimated on the basis of simultaneous measurements of CH_4 and C_2H_6 concentrations (Jackson et al., 2014; Fernandez et al., 2022). In Japan, the major gas companies in Tokyo and Osaka have stated that they supply natural gas with representative compositions of 89.6% CH_4 and 5.6% C_2H_6 (Tokyo) and 88.9% CH_4 and 6.8% C_2H_6 (Osaka). This suggests that natural gas leakage would simultaneously increase gas concentrations with a ratio of atmospheric concentration ($\Delta C_2H_6/\Delta CH_4$) of approximately 0.07 during downwind enhancement. Direct measurements of CH_4 and C_2H_6 fluxes should provide further information on the contributions of natural gas leakage in urban areas.

Eddy covariance (EC) methods are powerful tools for measuring spatially representative fluxes of greenhouse gases (Baldocchi, 2014). The EC method directly measures fluxes of trace gases between the land surface and atmosphere from the footprint upwind of the measurement point. The EC measurement represents a spatially integrated flux, where the flux footprint depends on the wind direction, height of the measurement, and atmospheric stability. The EC method has been used for measuring fluxes over terrestrial ecosystems (Baldocchi, 2014) but has been applied in urban areas to understand decade-long greenhouse gas emissions (Helfer et al., 2016; Liu et al., 2020; Ueyama and Takano, 2022). For urban areas, EC measurements have shown diurnal, seasonal and spatial variabilities in CO_2 fluxes in various cities (Helfer et al., 2016; Nordbo et al., 2012; Ueyama and Ando, 2016). Recently, CH_4 emissions have also been measured via the EC method in various cities (Gioli et al., 2013; Helfer et al., 2016; Pawlak and Fortuniak, 2016), which has demonstrated that urban areas are important CH_4 sources that are not fully characterized by the current inventories. Although the EC method provides spatially integrated fluxes, identifying detailed emission characteristics, such as the locations of emission hotspots and

https://doi.org/10.5194/egusphere-2024-3926
Preprint. Discussion started: 3 February 2025

source attributes (natural gas or biogenic sources), is difficult. Simultaneous EC and mobile measurements may provide additional insight into urban CH_4 emissions (Takano and Ueyama, 2021).

On the basis of a governmental inventory (NGGIDJ, 2024), CH_4 emissions from Japan decreased from 1.74×10^3 tCH_4 yr^{-1} in 1990 to 1.07×10^3 tCH_4 yr^{-1} in 2022. The contributions of CH_4 emissions to total greenhouse gas emissions are small (2.6% in 2022). Among the country-scale CH_4 emissions in 2022, the agricultural sector accounts for the most important CH_4 emission (81.9% of the total emission), and the waste sector (e.g., landfills, sewage plants) accounts for 12.1% of the emission. The leakage of natural gas is considered to be a minor CH_4 source (0.8%) in Japan. Although sophisticated emission datasets (Ito et al., 2019; NGGIDJ, 2024) have been developed and intensive field campaigns for rice paddies have been conducted (Itoh et al., 2011), urban CH_4 emissions have not been evaluated with atmospheric measurements in Japan.

In this study, we conducted mobile measurements of CH_4 and C_2H_6 fluxes and EC measurements of CH_4 fluxes to evaluate urban CH_4 emissions and their attributes in the metropolitan area of Osaka. Osaka is the second largest megacity in Japan and is therefore a priority target for characterizing urban CH_4 emissions. Our specific objectives are as follows:

1) Based on vehicle-based mobile measurements covering various urban areas from the city center to rural areas in Osaka Prefecture, can we understand emission characteristics on the basis of urban intensity?
2) Does the vehicle-mounted survey capture a true snapshot of an area's emission profile? We examine additional bicycle measurements that cover all streets within a target area for comparison.
3) Can mobile measurements be upscaled to provide estimates of regional CH_4 fluxes and compared with direct flux measurements via the EC method?
4) How does Osaka compare with other major international cities in terms of urban methane emissions abatement potential?

2. Method

2-1. Target area

The study area is the metropolitan area in Osaka, which is the second largest metropolitan area in Japan and includes two government-decreed cities: Osaka and Sakai. The population densities of Osaka and Sakai are 12,325 km^{-2} and 5,514 km^{-2}, respectively. The areas are highly urbanized. The total lengths of the roads within Osaka and Sakai are 3,712 km and 2,122 km, respectively. For natural gas distributions by a local gas company, the pipeline material for low-pressure gas is mostly polyethylene (PE), whose penetration is 89%. Other less prevalent materials include gray cast iron pipes, polyethylene lined steel pipes and galvanized steel pipes (https://www.daigasgroup.com/sustainability/). Approximately 96% of Osaka city sewer pipes use combined sewer systems, where both wastewater and stormwater flow through the same pipes. In Sakai city, only the northwest area (mostly Sakai Ward), which accounts for 12% of the city area, uses combined sewer systems.

https://doi.org/10.5194/egusphere-2024-3926
Preprint. Discussion started: 3 February 2025

2-2. Mobile measurements

We conducted two types of mobile measurements: vehicle and bicycle measurements. The vehicle measurements were intended to understand the characteristics of CH_4 emissions within Osaka Prefecture. The vehicle measurements were conducted along a gradient of urbanization from a dense city center in Osaka city, such as major commercial, business, and shopping districts (Umeda, Namba, and Tennoji), to rural areas in southern Sakai city. The bicycle measurements were conducted to cover all roads, including narrow streets that could not be driven by a vehicle, within the target area to ensure that almost no omissions occurred in the vehicle measurements and to clarify the overall picture of the emission sources within the area. The bicycle measurements were conducted mostly in Sakai, Kita, and Naka Wards of Sakai City.

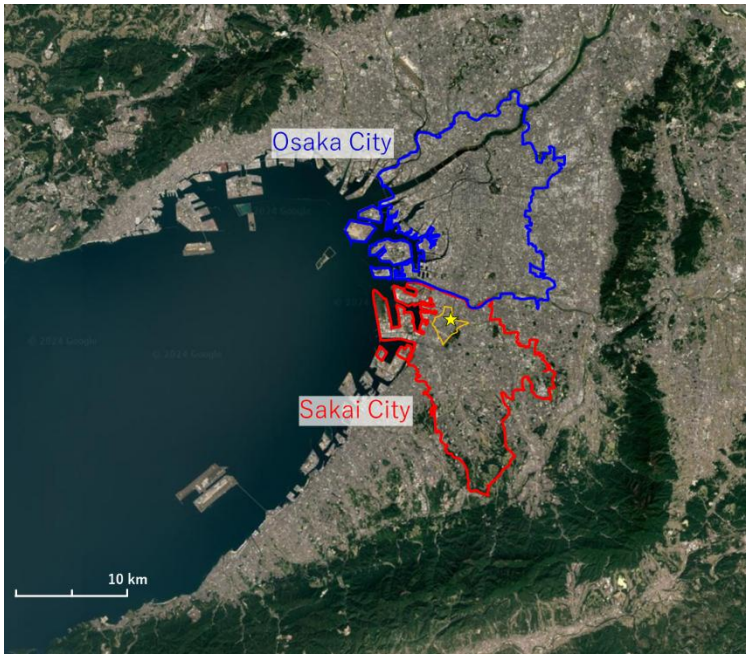

Fig. 1. Aerial map of the Osaka metropolitan area, where blue and red represent the boundaries of Osaka city and Sakai city, respectively. The yellow star represents the location of the eddy covariance tower, and the orange line represents the mean position of the source area contributing 80% to the flux footprint during the daytime (Ueyama and Takano, 2022). The map is obtained from Google Earth ©.

We conducted mobile measurements using a vehicle, mostly covering Osaka and Sakai cities (Fig. A1; Table A1). For each city, intensive mobile measurements were performed during the daytime on weekdays (Sep. 25–29, Nov. 13–17, 2023 for Sakai; Oct. 9–13, Dec. 11–15, 2023 for Osaka; Nov. 18–22, 2024 for Osaka). Additional mobile measurements using a vehicle were performed for coastal areas containing potential CH_4 hotspots, such as sewage plants and a landfill in Osaka Prefecture. Prior to the vehicle measurements, we set a target area each day, and the vehicle drove evenly on major roads and

https://doi.org/10.5194/egusphere-2024-3926
Preprint. Discussion started: 3 February 2025

small streets within the target areas where the vehicle could pass. In addition to this strategy, we also visited areas near known emission sources, such as sewage plants and dairy farms. To measure air near point sources, we conducted our observations in orbit around a potential point source if roads were publicly open; otherwise, we drove the roads closest to the source. Repeated observations were not conducted to prioritize observations of large areas, but several repeated observations were conducted for the dairy farm and the sewage plants in Sakai city. The total distance driven by the vehicle during the collection of measurements was 2,558 km: 1,280 km for Osaka city, 1,049 km for Sakai city, and 167 km for other cities. The mean vehicle speed each day was 17.0 ± 7.5 km hr^{-1}.

The vehicle measurements provided the CH_4, C_2H_6, and water vapor concentrations via a laser-based analyzer (MIRA Ultra, Aries Technologies, USA), the wind speed and direction via a sonic anemometer (Portable Mini, Calypso Instruments, USA), and the location via a global positioning system (GPS) (16X-HVS, Garmin, USA). These instruments were installed in a vehicle, and signals from the instruments were recorded via a datalogger (CR1000x, Campbell Scientific Inc., USA) at 1 second intervals. The inlet for the gas measurement was installed in the side door for the pavement side of the vehicle at 0.5 m above the ground. The height of the inlet was designed for effectively measuring CH_4 emissions from the ground (i.e., leakage from underground pipes). The additional CH_4 concentration measurements were conducted by a laser-based analyzer (LI-7810, LI-COR, USA), whose inlets were installed at the top of the vehicle roof (approximately 1.85 m above the ground), to examine differences in CH_4 emission detection at different measurement heights. The comparative LI-7810 and MIRA Ultra measurements were performed simultaneously over 25 days (Table A1). The sample air was drawn using a pump enveloped in the analyzer with a 0.4 liter per minute (LPM) flow rate. The lag times for the sampling were corrected in the analysis, which was determined by blowing air with a known CH_4 concentration into the inlet. Because the main purpose is to evaluate the origin of CH_4 emissions via simultaneous measurements of CH_4 and C_2H_6, unless otherwise stated, the CH_4 concentrations are those observed by MIRA Ultra.

Bicycle measurements were also conducted using a MIRA Ultra analyzer and a GPS embedded in the analyzer (Fig. A1). The CH_4 and C_2H_6 concentrations and locations were logged at 1-second intervals in the analyzer. An inlet for the gas sampling was located at the front of the bicycle (X3N-F8199-J4, Yamaha, Japan) at a height of 0.5 m above the ground, which is consistent with the vehicle measurement. The lag time between the inlet and the analyzer was corrected in the same manner as the vehicle measurements were. The mean bicycle speed each day was 9.7 ± 2.0 km hr^{-1}. The dates and travel distances of the bicycle measurements are shown in Table A2.

2-3. Eddy covariance measurements

The EC measurements were conducted at a 16-m tall tower at the top of the Sakai city center building (altitude of 112 m above the ground; 34.57°N, 135.48°E). For this tower site, we conducted long-term EC measurements of energy (Ando and Ueyama, 2017), water vapor (Ueyama et al., 2021), CO_2 (Ueyama and Ando, 2016; Ueyama and Takano, 2022), NO_2

https://doi.org/10.5194/egusphere-2024-3926
Preprint. Discussion started: 3 February 2025

(Okamura et al., 2024) and CH_4 (Takano and Ueyama, 2021) fluxes. The topography around the measurement area is flat. On the basis of flux footprint analysis (Takano and Ueyama, 2021; Fig. 1), the daytime fluxes, on average, represented 60% of the buildings, 22% of the roads, 13% of the vegetation and other land cover types. The region west of the tower comprises highly urbanized areas, including heavy traffic roads, highways, and coastal industrial regions, and the eastern region comprises mostly residential areas. Typical daytime flux footprints were included within the area measured by the bicycle. Two sewage plants surround the flux footprint in the western sector (Takano and Ueyama, 2021). Wind velocities were measured by a sonic anemometer (CSAT3, Campbell Scientific Inc., USA). CO_2 and water vapor densities were also measured via an open-path analyzer (EC150, Campbell Scientific Inc.), and CH_4 density was measured via an open-path analyzer (LI-7700, LI-COR, USA). The signals for turbulent fluctuations were recorded at 10 Hz via a data logger (CR1000X, Campbell Scientific, Inc.).

Turbulent fluxes were calculated via the EC method using the Flux Calculator program version 2 (Ueyama et al., 2012). Before calculating the covariance, spikes in the raw data were removed, and then a double-rotation method was applied to set the mean vertical wind velocity to zero. High-frequency attenuation was corrected on the basis of an empirical transfer function (Moore, 1986) for CH_4 fluxes, whereas the theoretical transfer function was applied for other fluxes. Air density correction was applied for CH_4 fluxes (McDermitt et al., 2011) and CO_2 and water vapor fluxes (Webb et al., 1980). Quality controls were applied via stationary tests and higher-moment tests (Vichers and Mahrt, 1997). Nighttime data were not filtered on the basis of the friction velocity (Ueyama and Takano, 2022). To prevent flow distortion by the tower, we did not use flux data when the wind direction was from the tower (45°－100°) (Okamura et al., 2024). Further details of the flux calculations are provided in previous studies (Takano and Ueyama, 2021; Ueyama and Takano, 2022).

To calculate daily and annual CH_4 fluxes, the data gaps were filled via the mean diurnal variation (MDV) method (Falge et al., 2001). Because the CH_4 fluxes were lower on weekends or holidays than on weekdays, the MDVs were determined separately for weekdays and weekends. To apply the MDV method, we used a 31-day moving window for weekdays and a 121-day moving window for weekends and holidays. The MDV method was conducted with 100 bootstrapping samples, and the mean and standard error of the bootstrapping were subsequently used for gap filling and their uncertainties, respectively. In this study, the measured fluxed from January 1 2023 to December 31 2023 were used for the analysis.

2-4. Water vapor corrections for the gas analyzer

According to a previous study (Commane et al., 2023), the gas analyzer used in this study requires a correction for the presence of water vapor. In this study, we used three analyzers of the same model (MIRA Ultra, Aries Technologies). We checked the response of the CH_4 and C_2H_6 concentrations to the water vapor concentration in the laboratory. The compressed air in the large-volume cylinders passed through the analyzer, and the water vapor concentration was changed by

https://doi.org/10.5194/egusphere-2024-3926
Preprint. Discussion started: 3 February 2025

dehumidifying or humidifying with Nafion tubing (ME-110, Perma Pure LLC, USA). We obtained the following empirical relationships for the CH_4 and C_2H_6 concentrations:

Analyzer 1

$$CH_4\,(H_2O) = -\,2.07786^{-10} * X_{H2O}^2 + 4.0952^{-6} * X_{H2O} - 0.020178 \quad (1)$$

Analyzer 2

$$CH_4\,(H_2O) = -\,3.2856^{-10} * X_{H2O}^2 + 8.4828^{-6} * X_{H2O} - 0.05478 \quad (2)$$

$$C_2H_6\,(H_2O) = 4.8243^{-5} * X_{H2O} - 0.6521 \quad (3)$$

Analyzer 3

$$CH_4\,(H_2O) = 2.11169^{-11} * X_{H2O}^2 - 1.42907^{6} * X_{H2O} - 0.020178 \quad (4)$$

where X_{H2O} represents the water vapor concentration (ppm). $CH_4\,(H_2O)$ and $C_2H_6\,(H_2O)$ are the changes in the CH_4 and C_2H_6 concentrations, respectively, as a function of the water vapor concentration. For the mobile and atmospheric measurements, we corrected the effect of water vapor to values at water vapor concentrations of 10,000 ppm for analyzers 1 and 3 and 13,000 ppm for analyzer 2. For the C_2H_6 concentration, we only found a clear linear increase in water vapor for analyzer 2; water vapor correction was applied for analyzer 2 only, where the C_2H_6 value was corrected to 13,000 ppm water vapor.

2-5. Data analysis for mobile measurements

The CH_4 emission hotspots were identified via the data from the mobile measurements. For both the vehicle and bicycle measurements, hotspots were defined as locations where the CH_4 concentration was elevated by more than 0.1 ppm with respect to the local baseline concentration (hereafter referred to as CH_4 enhancement; ΔCH_4). The local background concentration was defined as the 5th percentile value during a 5-minute moving window (i.e., a 2.5-minute window on either side of a measurement point). In addition to ΔCH_4, the C_2H_6 enhancement (ΔC_2H_6) was calculated in the same manner and was used for estimating the source attributions of ΔCH_4. In accordance with a previous study that used the C_2H_6:CH_4 (C_2:C_1) ratio (Fernandez et al., 2022), we grouped the CH_4 hotspots into three categories: biogenic (C_2:C_1 < 0.005), natural gas (0.005 < C_2:C_1 < 0.1), and combustion (C_2:C_1 > 0.1) sources. Although the C_2:C_1 ratio for the natural gas distribution in Osaka is reported to be 0.076, we used a wider range of C_2:C_1 ratios for the source attributed to natural gas owing to potential dilution by surrounding air. For the vehicle measurements, we eliminated the data when the vehicle speed was less

https://doi.org/10.5194/egusphere-2024-3926
Preprint. Discussion started: 3 February 2025

than 1.5 km hr^{-1} to prevent possible contamination from vehicle exhaust during idling. The identified CH_4 enhancements were aggregated with a spatial resolution of 12 s (approximately 37 m) by obtaining the maximum CH_4 enhancement (hereafter referred to as a leak indication, LI) to avoid double counting of surrounding LIs. On the basis of the mean speed of the vehicle (17.0 km hr^{-1}) and bicycle (9.7 km hr^{-1}), approximately 7.8 and 13.7 measurement points were, on average, available for the vehicle and bicycle measurement analysis, respectively, within the 37-m spatial resolution.

To categorize the CH_4 LI intensity, we employed the emission magnitude categories defined in previous studies (Fernandez et al., 2022; von Fisher et al., 2017): low emissions (< 6 L min^{-1}), medium emissions (6--6–40 L min^{-1}), and high emissions (> 40 L min^{-1}). The emission rate was calculated via Eq. 5. These emission categories correspond to CH_4 enhancements of low emissions (< 1.6 ppm), medium emissions (1.6 to 7.6 ppm), and high emissions (7.6 ppm) in the empirical model by Weller et al. (2019). We found that it underestimated the regional CH_4 fluxes in the empirical model, as noted below. Consequently, the use of units in the emission rate might be misleading; therefore, we used the unit of CH_4 enhancement (i.e., ppm) but a definition consistent with that used in previous studies.

To estimate regional CH_4 emissions on the basis of mobile measurements, we used an empirical equation (Weller et al., 2019) with a correction applied to ensure that the upscaled CH_4 fluxes were consistent with the daytime CH_4 fluxes from the EC measurements. Despite this simplification, our objectives are to 1) identify leaks and determine associated CH_4 emissions in Osaka and 2) compare CH_4 emissions in a Japanese city with those in other cities whose CH_4 emissions are calculated via this equation (Vogel et al. 2024). In accordance with Weller et al. (2019), the CH_4 emission rate was calculated as follows:

$$\ln(Em) = (\ln(C) + 0.988)/0.817) \quad (5)$$

where Em is the emission rate (L min^{-1}) and where C is the maximum CH_4 LI (ppm) within a grid. Here, Em was calculated on the basis of C measured by a gas analyzer (Mira Ultra) at 0.5 m instead of another gas analyzer (LI-7810) at 1.85 m. Using Em, the CH_4 fluxes were calculated as follows:

$$F_{ch4} = A \times Em_{mean} \times Num \times Dist/Area \quad (6)$$

where F_{ch4} represents the CH_4 fluxes (nmol m^{-2} s^{-1}), Em_{mean} represents the areal mean of Em, Num represents the detected hotspot count per travel distance (km^{-1}), $Dist$ represents the total road length of the target ward or city (km), $Area$ represents the area of the target ward or city (m^2), and A represents the correction factor of the empirical estimates. For the total road length, we did not include the length of highways because highways are generally located over or along arterial roads. To account for uncertainties associated with limited measurements, Em_{mean} was calculated 100 times via bootstrap sampling from the measurements, and the mean and standard deviation of F_{ch4} were calculated from 100 bootstrapped samples. Eq. (5)

https://doi.org/10.5194/egusphere-2024-3926
Preprint. Discussion started: 3 February 2025

was applied to calculate F_{ch4} for each ward or city. This upscaling procedure was conducted for the respective biogenic and natural gas LIs and then summed for each flux. We did not upscale the combustion LIs because combustion was identified as a minor source of CH_4 in the measured data. The total flux calculation was also performed for all LIs (not categorized). CH_4 fluxes upscaled by the two estimates (with and without source attributions) were compared to understand the uncertainties associated with the procedure.

On the basis of the comparison between the F_{ch4} values calculated with A = 1.0 and the mean daytime CH_4 fluxes from the EC measurements, we found that the upscaled CH_4 fluxes for Sakai Ward were substantially underestimated, even considering the run-by-run variations in the EC-based daytime CH_4 fluxes. Consequently, we set A to 22 to account for the underestimates. To determine the A factor, we used bicycle measurements, which covered almost all streets of Sakai Ward and were roughly consistent with the climatological mean of the daytime flux footprint of the EC measurement. The assumption of the correction was that the CH_4 flux determined via the top-down method (i.e., the EC method) was attributed completely to the CH_4 emissions detected via mobile measurements. This assumption might contain considerable uncertainties because there could be potential sources in tall buildings or roofs. However, considerable underestimates in Eq. 5 might cause a mismatch in a Japanese city. This correction factor was also applied to calculate F_{ch4} for other regions via bicycle and vehicle measurements. We discuss the uncertainties in later sections.

To understand the uncertainties in upscaled regional fluxes, we further examined the different equations proposed by recent studies after Weller et al. (2019). Instead of using Eq. 5, the following equations were applied for evaluating CH_4 emissions:

$$\ln(Em) = (\ln(C) + 0.521)/0.795) \quad (7)$$

$$\ln(Em) = (\ln(C) + 2.738)/1.329) \quad (8)$$

$$\ln(Em) = (\ln(C) + 2.716)/0.741) \quad (9)$$

Three equations were developed on the basis of a control experiment in Germany (Weitzel and Schmidt, 2023), South Korea (Joo et al., 2024), and Japan (Umezawa et al., in preparation). For calculating fluxes, the correction factor, A, was similarly determined: A = 38 for Eq. 7, A = 10 for Eq. 8, and A = 1.9 for Eq. 9. The different estimates of Em and associated differences in A could be caused by assumptions made in the control experiments. We estimated the upscaled CH_4 fluxes via Eqs. 5, 7, 8, and 9 and considered the range of upscaled fluxes as an uncertainty.

Upscaled CH_4 fluxes were aggregated at the ward or city scale for Sakai city and Osaka city. Fluxes from the vehicle and bicycle measurements were compared for Kita and Sakai Wards of Sakai city, as well as for Sakai city. The comparison of

https://doi.org/10.5194/egusphere-2024-3926
Preprint. Discussion started: 3 February 2025

CH_4 fluxes for Kita and Sakai Wards could provide insight into how the coarse vehicle measurements were consistent with the intensive bicycle measurements that covered almost all streets. A comparison of CH_4 fluxes across Sakai city was conducted to assess how city-scale CH_4 fluxes differ in terms of spatial coverage between vehicle measurements (covering various urban landscapes) and bicycle measurements (covering only city center and residential areas).

The total CH_4 emissions were calculated by multiplying the upscaled CH_4 fluxes to the city area and a factor for the temporal representation. Although mobile measurements were conducted in the daytime, we found that the CH_4 fluxes obtained via the EC method (Takano and Ueyama, 2021) clearly exhibited diurnal variation. To consider the diurnal variability, we multiplied the upscaled fluxes by 0.64 when calculating the daily fluxes. The daily fluxes were then summed over 365 days for the annual fluxes because CH_4 emissions during the seasons of Oct. and Nov. when the mobile measurements were conducted were similar to the annual mean (later discussed with Fig. 10f). The annual emissions were only calculated for the vehicle measurements because the bicycle measurements were only conducted for the city center and residential areas and might underrepresent the rural areas.

On the basis of visual inspections of mobile measurement data, many LIs have been detected near restaurants. We quantified whether LIs were significantly more common near restaurants than others were. First, the probability of detecting restaurants near LIs, P(R|LI), was calculated, where the locations of the restaurants were obtained via two databases on gourmet websites: Yahoo (https://developer.yahoo.co.jp) and Hot Pepper Gourmet by Recruit (https://www.hotpepper.jp/). To use the databases, we used an application programming interface (API) provided by the companies. Because the two available databases did not fully cover all restaurants in the cities, we compared the probability that the CH_4 concentration significantly increased near restaurants. We identified whether restaurants were located within 80 m from an LI, and then the probability was calculated for Sakai city and Osaka city. The distance of 80 m was determined on the basis of visual inspection, considering the precision of the restaurant location in the database and the distance between roads and buildings. Then, a baseline probability was determined on the basis of 5 bootstrapping samples of randomly selected points that were not identified as an LI (i.e., the probability of a restaurant being within 80 m given that there is no detection, P(R|no LI)). Finally, we compared the probability of restaurants being located near LIs to that of the baseline. On the basis of Bayesian theory, we calculate the inverse probability of P(R|LI), namely, the probability that restaurants emit natural gas related to CH_4, P(LI|R), as follows:

$$P(LI|R) = P(R|LI) \times P(LI)/P(R) \quad (9)$$

$$P(R) = P(R|LI) \times P(LI) + P(R|\text{no LI}) \times P(\text{no LI}) \quad (10)$$

https://doi.org/10.5194/egusphere-2024-3926
Preprint. Discussion started: 3 February 2025

where P(R) is the probability of existing restaurants within the 80 m sector, P(LI) is the probability of LIs existing within the 80 m sector, and P(no LI) is the probability of no LIs existing within the 80 m sector.

Differences in CH_4 enhancements between the two types of gas analyzers at different heights were evaluated via vehicle measurements. On the basis of previous studies (von Fischer et al., 2017; Weller et al., 2019), CH_4 emissions are expected from underground pipes used in natural gas distribution. Furthermore, wind speeds are generally lower at lower measurement heights, resulting in less diluted emission plumes. Considering these assumptions, our high-priority gas measurements were performed at 0.5 m using a gas analyzer (Mira Ultra; the optical cavity is 60 cm^3), but the measurements for 1.85 m were simultaneously examined with an LI-7810 analyzer (optical cavity is 6.41 cm^3). We compared LIs with the two measurements to assess which heights effectively detected LIs.

3. Results

3-1. Vehicle measurements

On the basis of the vehicle measurements, we surveyed 2,558 km across the Osaka metropolitan area, mostly in Osaka city (1,280 km) and Sakai city (1,049 km), and identified 753 LIs (Fig. 2). Among the LIs, 233 LIs were classified as biogenic sources, and 481 LIs were classified as natural gas sources. Pyrogenic sources were minor for our measurements (39 LIs). Ninety-five percent of the detected LIs were less than 1 ppm in enhancement, indicating that the detected LIs were mainly small leaks. Scatter plots between the CH_4 and C_2H_6 enhancements revealed that many of the CH_4 enhancements increased with increasing C_2H_6 concentration according to the gas supply ratio set by the local gas company (C_2:C_1 = 0.076 ppm ppm^{-1}) (Fig. 3a). Furthermore, the data with a high C_2:C_1 ratio were highly correlated at the local scale, where the red dots in Fig. 3 represent correlation coefficients between the two gases that were greater than 0.7 for the 5-min timeframe. These results indicate that LIs that originate from a natural gas source can be correctly classified via C_2H_6. On the basis of visual inspection and smell during measurements near CH_4 enhancements, the interpretable reasons for CH_4 enhancement were sewage plants, sewer pipes, plants for fermented foods, reservoirs, ditches of kofun (monument of an ancient emperor), river sides, dairy farms, composts, industrial plants, and various types of restaurants, including market streets. Unattributable enhancements were also measured in various land uses, such as residential, commercial and industrial areas.

https://doi.org/10.5194/egusphere-2024-3926
Preprint. Discussion started: 3 February 2025

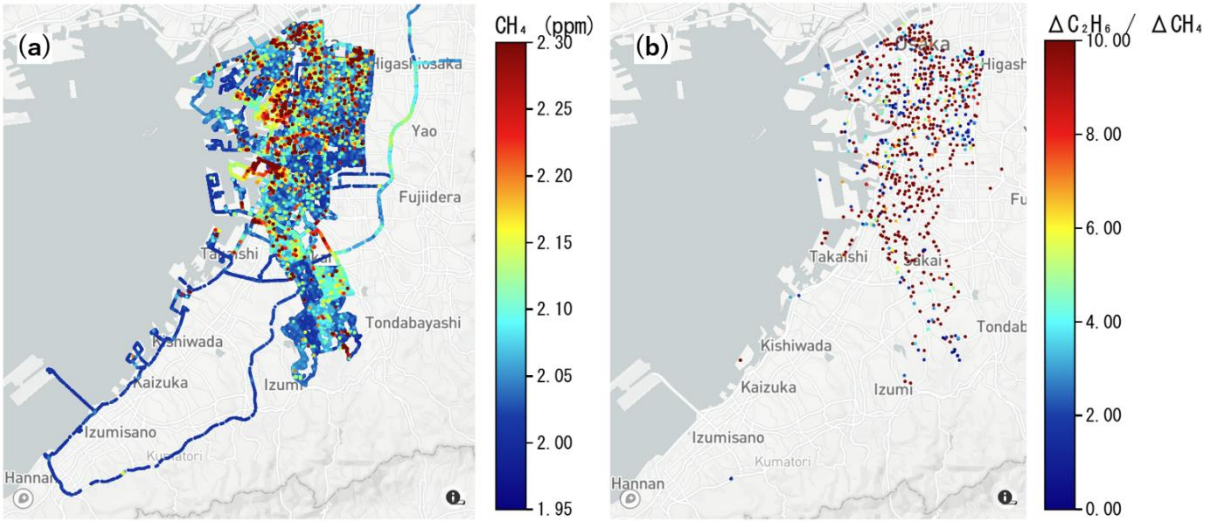

Fig. 2. Spatial distributions of CH_4 concentrations (a) and identified leak indications (LIs) (b) on the basis of vehicle measurements. The color bar scale in b is the C_2:C_1 ratio (ppb ppm^{-1}). Visualisation was achieved by the ploty in python which uses OpenStreetMap© as a basemap provided by mapbox©.

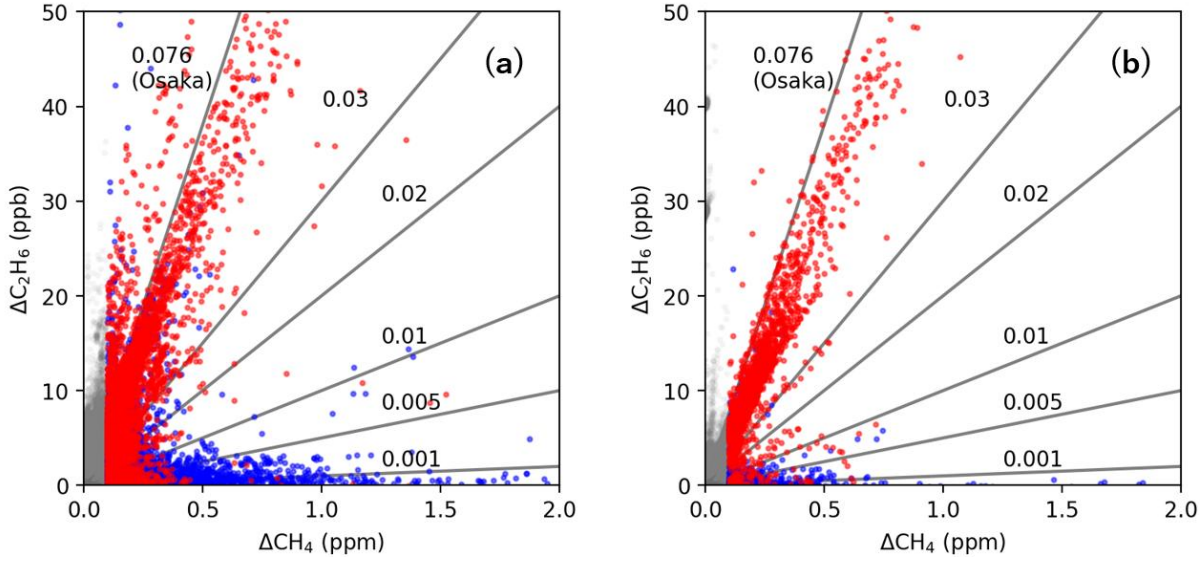

Fig. 3. Relationships between CH_4 and C_2H_6 enhancements based on vehicle measurements (a) and bicycle measurements (b). The red dots represent the data for which the correlation coefficient between these two gases was greater than 0.7, and the blue dots represent the data for which the correlation coefficient was lower. The lines represent various slopes, and 0.076 ppm ppm^{-1} represents the C_2:C_1 ratio for natural gas provided by the local gas company in the Osaka metropolitan area.

https://doi.org/10.5194/egusphere-2024-3926
Preprint. Discussion started: 3 February 2025

LIs per travel distance were 2 times greater in Osaka city (495 LIs; 0.39 km^{-1}) than in Sakai city (235 LIs; 0.22 km^{-1}). In terms of emission sources, both biogenic and natural gas LIs were higher in Osaka city (0.13 km^{-1} for biogenic gas and 0.24 km^{-1} for natural gas) than in Sakai city (0.05 km^{-1} for biogenic gas and 0.15 km^{-1} for natural gas). These results indicate that Osaka city, which is more urbanized than Sakai city is, has more natural gas and biological CH_4 emission points.

The intensities of LIs were generally low, where 733 LIs out of 753 LIs (i.e., 97.3%) were classified into a low category (i.e., less than 1.6 ppm enhancement) (Fig. 4). There was no high-emission category (i.e., greater than 7.6 ppm enhancement) in Osaka and Sakai cites. Twenty LIs were categorized as middle. The highest LI (7.57 ppm enhancement) was observed near compost in croplands in the rural area of Sakai city, which was identified as a biogenic source. The second to fourth highest enhancements (6.5 to 5.4 ppm, respectively) were natural gas sources in Osaka city, which were observed at a narrow street in a residential area or at a main street in a commercial area. The second highest biological enhancement (4.39 ppm) was detected in the bay area.

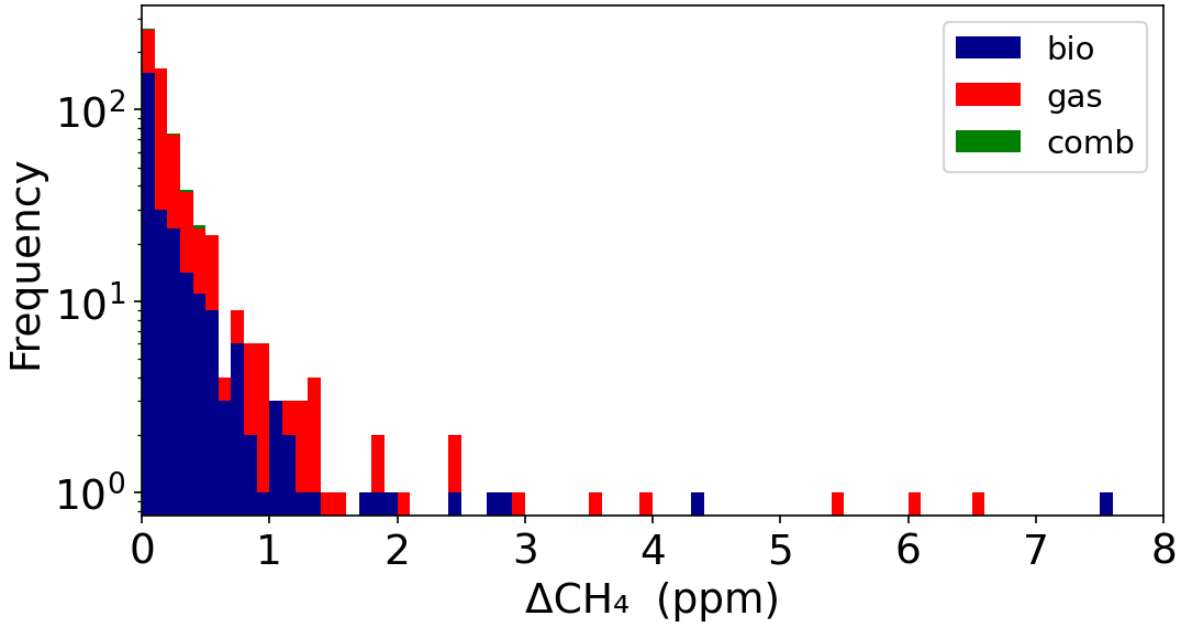

Fig. 4. Histogram of CH_4 enhancements (ΔCH_4) based on vehicle measurements for Osaka and Sakai. Note that the y-axis is shown as a log scale.

The detected numbers of LIs and ΔCH_4 were greater in the Ultra gas analyzer, whose inlet was installed at 0.5 m, than in the LI-7810 analyzer, whose inlet was installed at 1.85 m (Fig. A2), where comparisons were made when the CH_4 concentrations were measured by both analyzers. The estimated LIs were 723 for Osaka and Sakai cities in terms of the

https://doi.org/10.5194/egusphere-2024-3926
Preprint. Discussion started: 3 February 2025

measurements by the Ultra analyzer, but those by the LI-7810 analyzer were 646. The underestimation of the number of LIs by the LI-7810 analyzer was more significant for biological sources (130 for LI-7810 and 221 for Ultra) than for natural gas sources (370 for LI-7810 and 468 for Ultra). Combustion sources were also more effectively detected by the Ultra analyzer (34) than the LI-7810 analyzer (6). The maximum and median ΔCH_4 values were 7.6 ppm and 0.20 ppm, respectively, for the Ultra analyzer, whereas those for the LI-7810 analyzer were 3.4 ppm and 0.14 ppm, respectively.

3-2. Bicycle measurements

The bicycle measurements provided characteristics similar to those obtained from the vehicle measurements (Fig. 5). The bicycle measurements provided a detailed view of CH_4 concentrations and LIs with high density, which covered almost all streets, including very narrow streets and deadends that could not be accessed by a vehicle (Fig. A3). Many CH_4 enhancements were evident in the C_2:C_1 ratio according to the local natural gas company (Fig. 3b), which was consistent with the vehicle measurements (Fig. 3a).

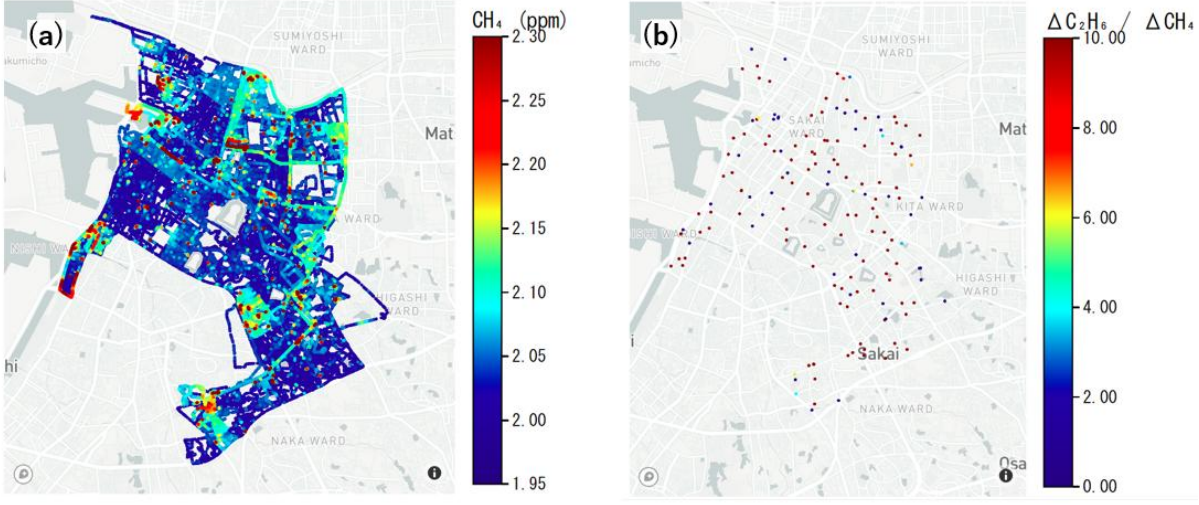

Fig. 5. Spatial distributions of CH_4 concentrations (a) and identified leak indications (LIs) (b) on the basis of bicycle measurements. To remove the daily variations in the CH_4 concentration for visualization, the CH_4 concentrations were rescaled so that the 5th percentile of the CH_4 concentration on each measurement day was 2.0 ppm; this rescaling was performed only for visualization and not as part of the data processing and analysis. Visualisation was achieved by the ploty in python which uses OpenStreetMap© as a basemap provided by mapbox©.

The number of identified LIs was 187 per 1,162 km from the north to the central part of Sakai city (Fig. 6). The LI density (0.16 km^{-1}) was similar to that obtained from the vehicle measurements for the same area (0.25 km^{-1} when including combustion LIs or 0.23 km^{-1} when not including combustion LIs). Compared with the vehicle measurements (64%), the

https://doi.org/10.5194/egusphere-2024-3926
Preprint. Discussion started: 3 February 2025

percentage of natural gas CH_4 LIs (75%) was greater in the bicycle measurements than in the vehicle measurements. As with the vehicle measurements, there was no LI categorized as high, and 181 LIs out of 187 LIs were categorized as small. The highest LI was 5.9 ppm, which was identified as a biogenic source near a fermented food factory. The second and third highest LIs were observed near a building at Osaka Metropolitan University (4.3 ppm enhancement) and at a narrow street in a residential area (4.2 ppm enhancement), respectively, which were identified as natural gas sources. There was no LI categorized as combustion on the basis of the bicycle measurements.

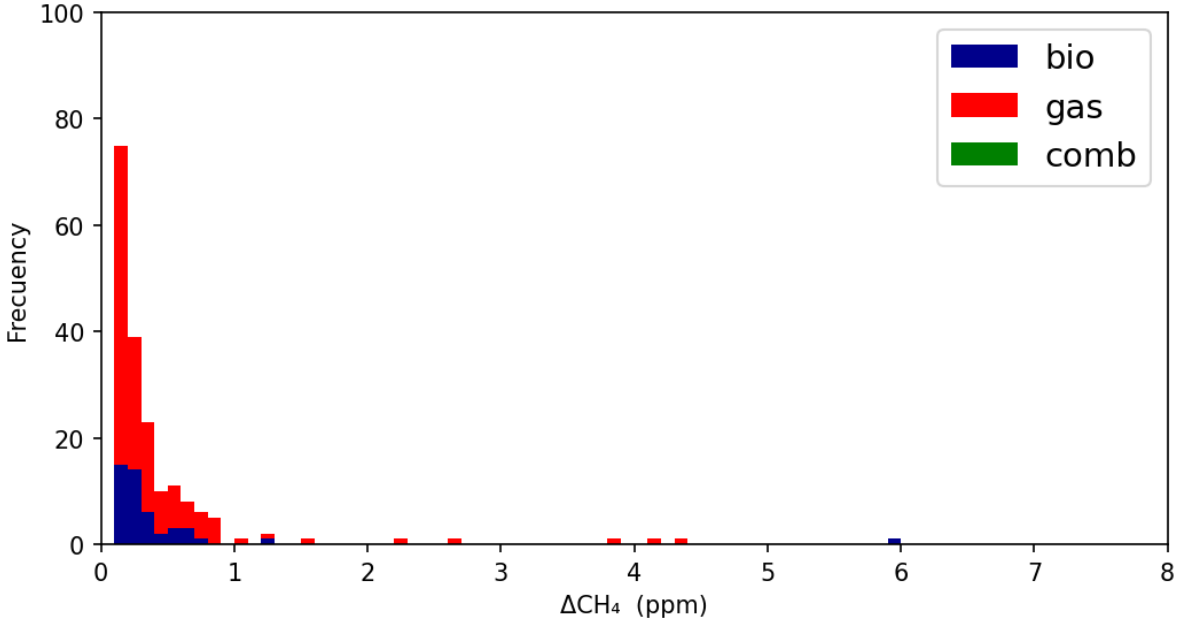

Fig. 6. Histogram of CH_4 enhancements (ΔCH_4) based on bicycle measurements for Osaka and Sakai.

3-3. Regional CH_4 fluxes and emissions

On the basis of the detected LIs with the empirical equations (Eqs. 5 to 9), CH_4 fluxes were estimated for the administrative divisions of Sakai city to compare the fluxes determined from the bicycle and vehicle measurements. Notably, the estimated CH_4 fluxes were calibrated to ensure that the upscaled CH_4 fluxes for Sakai Ward from the bicycle measurements were consistent with the long-term mean daytime CH_4 fluxes measured via the EC method (approximately 65 nmol m^{-2} s^{-1}) (Sections 2–5 and 3–5). There was no clear difference in CH_4 flux between estimates based on the sum of biological and natural gas fluxes and direct estimates without considering the source types (Fig. 7).

The estimated CH_4 fluxes for Sakai city were 51 ± 5 nmol m^{-2} s^{-1} according to the bicycle measurements and 49 ± 10 nmol m^{-2} s^{-1} according to the vehicle measurements. Hereafter, the value and plus/minus sign of the regional flux represent the

https://doi.org/10.5194/egusphere-2024-3926
Preprint. Discussion started: 3 February 2025

mean and standard deviation of the fluxes upscaled by four different equations (Eqs. 5, 7, 8, and 9), respectively. Both estimates were generally similar, although different spatial representations and densities of the measurements were used. The bicycle measurements did not cover Minami and Mihara Wards completely and covered only a few km for Higashi and Nishi Wards. In contrast, vehicle measurements were missing data for only Mihara Ward. In addition to the city-scale fluxes, fluxes for each ward were also consistent between the bicycle and vehicle measurements, except for Kita Ward, where CH_4 fluxes were lower in the vehicle measurements (35 ± 15 nmol m^{-2} s^{-1}) than in the bicycle measurements (50 ± 7 nmol m^{-2} s^{-1}).

Although the total fluxes were consistent between the bicycle and vehicle measurements, the components of the fluxes, namely, the biogenic and natural gas fluxes, differed (Fig. 7). The biogenic fluxes were greater in the vehicle measurements than in the bicycle measurements, whereas the natural gas fluxes were the opposite. On the basis of the bicycle measurements, the biogenic and natural gas CH_4 fluxes for Sakai city were 13 ± 1 nmol m^{-2} s^{-1} and 38 ± 4 nmol m^{-2} s^{-1}, respectively, indicating that natural gas fluxes explained 75% of the total CH_4 flux. For vehicle measurements, natural gas fluxes explained 47% of the total CH_4 flux: 25 ± 1 nmol m^{-2} s^{-1} for biogenic fluxes and 23 ± 9 nmol m^{-2} s^{-1} for natural gas fluxes.

Among Sakai, Naka, and Kita Wards, which were measured via both bicycle and vehicle measurements, biogenic fluxes tended to have greater contributions in Sakai Ward than in the other wards, which was consistent between the two measurements. The high contributions of biogenic sources could be explained by the combined sewer systems that remain in Sakai Ward but not in other wards in Sakai city. Furthermore, this result may be explained by the presence of Sakai city's largest sewage treatment plant in Sakai Ward. The high contributions of biogenic fluxes in Minami Ward (Fig. 7b) were associated with CH_4 fluxes from compost, dairy farms, and reservoirs because Minami Ward is the most rural place in Sakai city. For Nishi Ward, the bicycle measurements underrepresented the CH_4 fluxes owing to collecting data over 62 km.

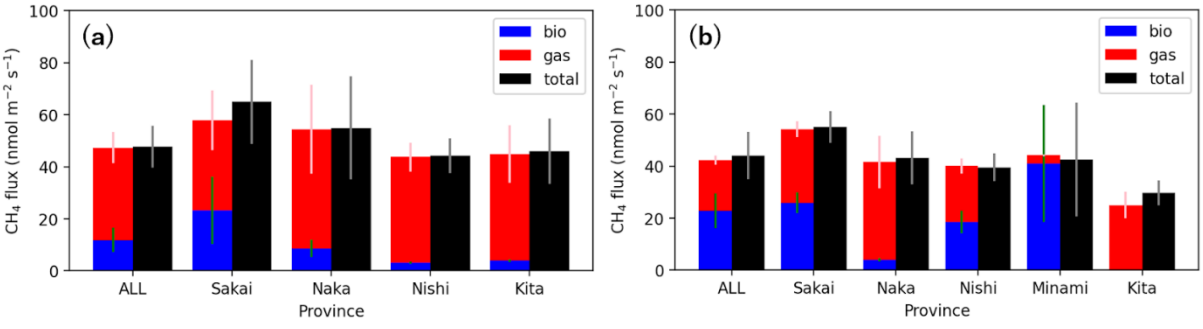

Fig. 7. Upscaled CH_4 fluxes for Sakai city in terms of the entire city and each ward based on the bicycle measurements (a) and the vehicle measurements (b) using Eq. (4). The error bars represent the standard deviation based on bootstrapped samples.

https://doi.org/10.5194/egusphere-2024-3926
Preprint. Discussion started: 3 February 2025

The upscaled CH_4 fluxes for Osaka city (138 ± 14 nmol m^{-2} s^{-1}) were 2.8 times greater than those for Sakai city (Fig. 8). The four high CH_4 fluxes were estimated for Fukushima, Higashinari, Joto, and Hirano Wards. Fukushima Ward is the commercial and industrial area near Umeda station, the largest train station in Osaka Prefecture. Fukushima Ward has the second largest sewage plant in terms of treatment capacity (326,000 m^3 d^{-1}) in Osaka city. Joto and Higashinari Wards are the second (29,183 km^{-2}) and third (18,727 km^{-2}) most densely populated areas in Osaka Prefecture. Except for Konohana and Tennoji Wards, the CH_4 fluxes in wards in Osaka city were higher than those in Sakai city. For Osaka city, biogenic and natural gas fluxes contributed almost equally to the total CH_4 fluxes. On the basis of the vehicle measurements, the contributions of natural gas fluxes were greater in Osaka city (64%) than in Sakai city (47%).

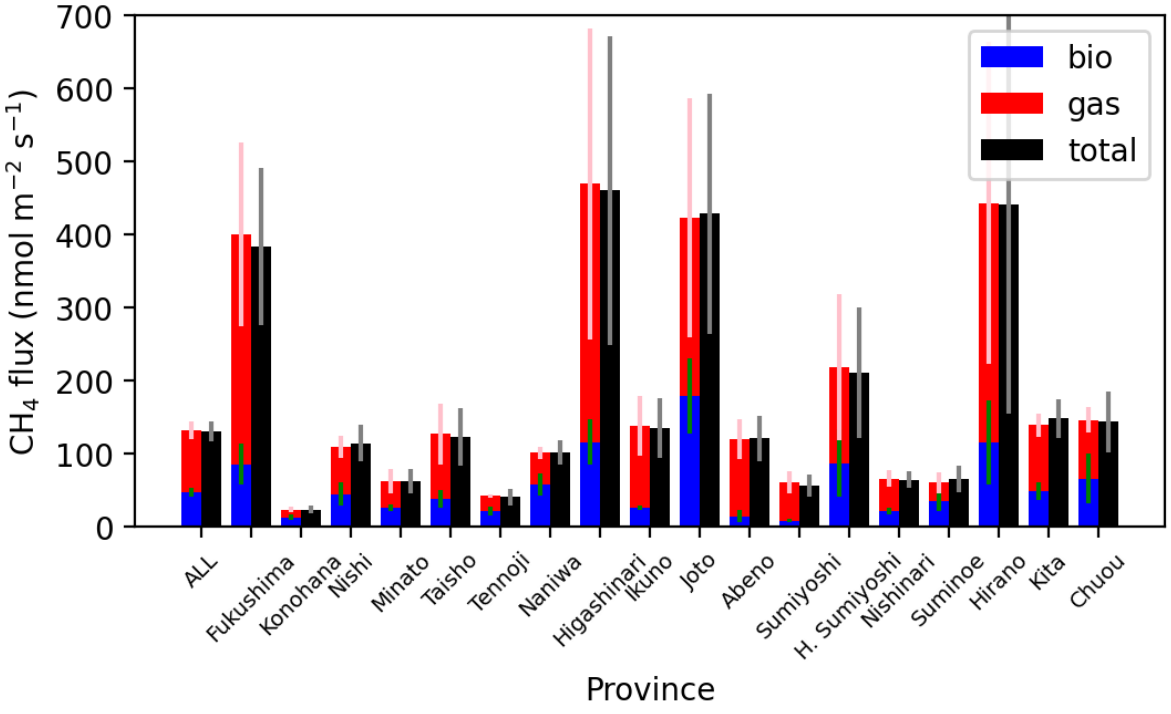

Fig. 8. Upscaled CH_4 fluxes for Osaka city in terms of the entire city and each ward based on bicycle measurements using Eq. 6. The error bars represent the standard deviation based on bootstrapped samples.

The scaled annual CH_4 emissions, which were calculated via the CH_4 fluxes, the area of the city, and temporal correction, resulting in 10,021 ± 1,000 tCH_4 yr^{-1} for Osaka city and 2,379 ± 480 tCH_4 yr^{-1} for Sakai city on the basis of the vehicle measurements. These values were equivalent to the annual area-weighted fluxes of 44 ± 4 tCH_4 km^{-2} yr^{-1} for Osaka city and 16 ± 3 tCH_4 km^{-2} yr^{-1} for Sakai city. The biological emissions were 3,632 ± 480 tCH_4 yr^{-1} for Osaka city and 1191 ± 47 tCH_4

https://doi.org/10.5194/egusphere-2024-3926
Preprint. Discussion started: 3 February 2025

yr^{-1} for Sakai city, whereas the natural gas emissions were 6,389 ± 520 tCH_4 yr^{-1} for Osaka city and 1,188 ± 433 tCH_4 yr^{-1} for Sakai city. It is worth noting that the annual emissions corrected the flux ratio between the daytime mean and daily mean (0.64) on the basis of the magnitude of the CH_4 fluxes measured via the EC method (Sections 2--2–5).

3-4. Restaurants and sewage plants

The probability of a restaurant existing near identified natural gas LIs was significantly greater than that near a location where no natural gas LI was observed (hereafter referred to as the baseline probability) (Fig. 9). For Sakai city, the probability of a restaurant being included in the vehicle measurements was 14%, and the probability of a restaurant being included in the bicycle measurements was 20%, which was significantly greater than the baseline probability (4.7% ± 0.8% for the vehicle measurements and 8.8 ± 0.4% for the bicycle measurements; plus/minus sign denotes standard error of bootstrapping). The probability of a restaurant existing near natural gas LIs was 30% for Osaka city, which was higher than that for Sakai city. The baseline probability for Osaka city (22% ± 1.4%) was also higher than that for Sakai city because Osaka city is a highly urbanized city where there are many restaurants. On the basis of Bayesian theory, the probabilities of existing restaurants emitting natural gas-related CH_4 were 2.4% for Osaka city, 2.5% for Sakai city according to vehicle measurements and 2.7% for Sakai city according to bicycle measurements. This finding either suggests that 2–3% of restaurants have detectable gas leaks or that if all restaurants emit CH_4, they only emit detectable levels (detectable at the roadside) 2–3% of the time.

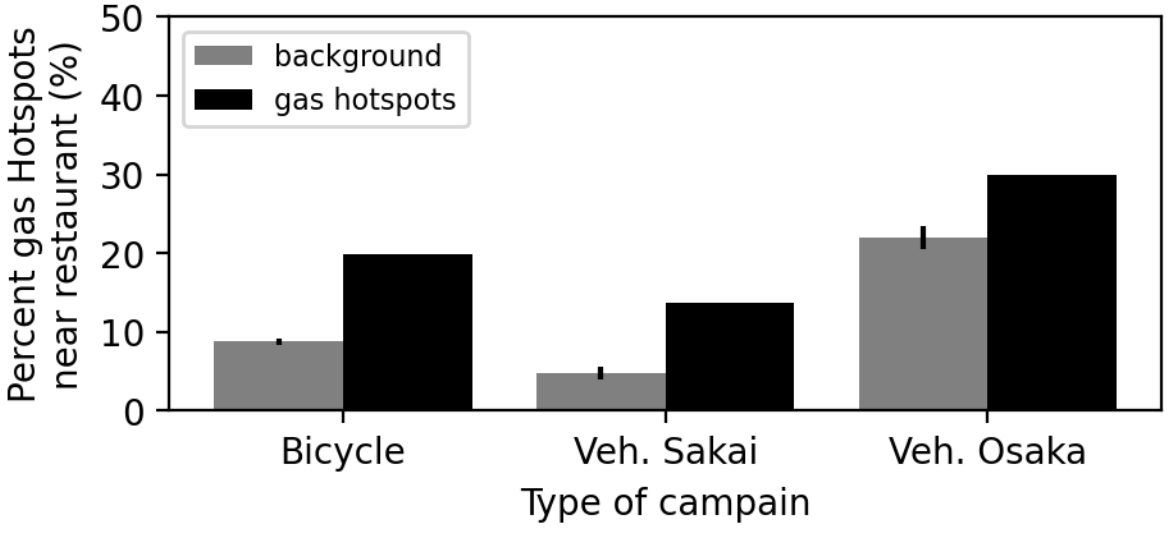

Fig. 9. Probability of a restaurant existing near identified natural gas LIs and that near a location where no natural gas LI was identified. The error bars represent the standard errors for bootstrapped samples randomly obtained from the mobile measurement data where natural gas LIs were not identified.

https://doi.org/10.5194/egusphere-2024-3926
Preprint. Discussion started: 3 February 2025

CH_4 enhancements near sewage plants were not too high, i.e., up to 4.3 ppm (Fig. A4). Although the C_2:C_1 ratio revealed that most of the CH_4 enhancements were biological (n = 11), 4 plants with high C_2:C_1 ratios (Chisima, Nakahama, Tsumori, and Chubu Mizumirai) were classified as having natural gas emissions.

3-5. Eddy covariance measurements

The CH_4 fluxes measured via the EC method clearly exhibited diurnal variations throughout the seasons (Fig. 10). The daytime CH_4 emissions were higher than the nighttime CH_4 emissions throughout the seasons. CH_4 emissions were higher in the western sector than in the eastern sector, possibly because these sectors are associated with high human activities (Ueyama and Ando, 2016) and sewage plants (Takano and Ueyama. 2021). For the western sector, the daytime emissions in spring (Fig. 10a) were lower than those in the other seasons. The daytime CH_4 emissions in the western sector were, on average, 68 nmol m^{-2} s^{-1} in the autumn and winter periods, when most of the mobile measurements were collected. The seasonal variations in CH_4 fluxes showed two peaks, where summer emissions were highest and a smaller peak occurred in winter (Fig. 10f). The CH_4 fluxes were greater on weekdays (46 nmol m^{-2} s^{-1}) than on weekends and holidays (34 nmol m^{-2} s^{-1}), especially during the daytime (72 nmol m^{-2} s^{-1} on weekdays and 50 nmol m^{-2} s^{-1} on weekends and holidays) (Fig. 10e). The annual CH_4 emissions in 2023 according to the EC measurements were 14.2 ± 1.3 g CH_4 m^{-2} yr^{-1} (plus/minus sign represents the standard error). The annual emissions in 2023 according to the EC measurements were close to those obtained from the mobile measurements accounting for the *A* factor in Sakai city on the basis of both bicycle measurements (16 ± 2 g CH_4 m^{-2} yr^{-1}) and vehicle measurements (16 ± 3 g CH_4 m^{-2} yr^{-1}).

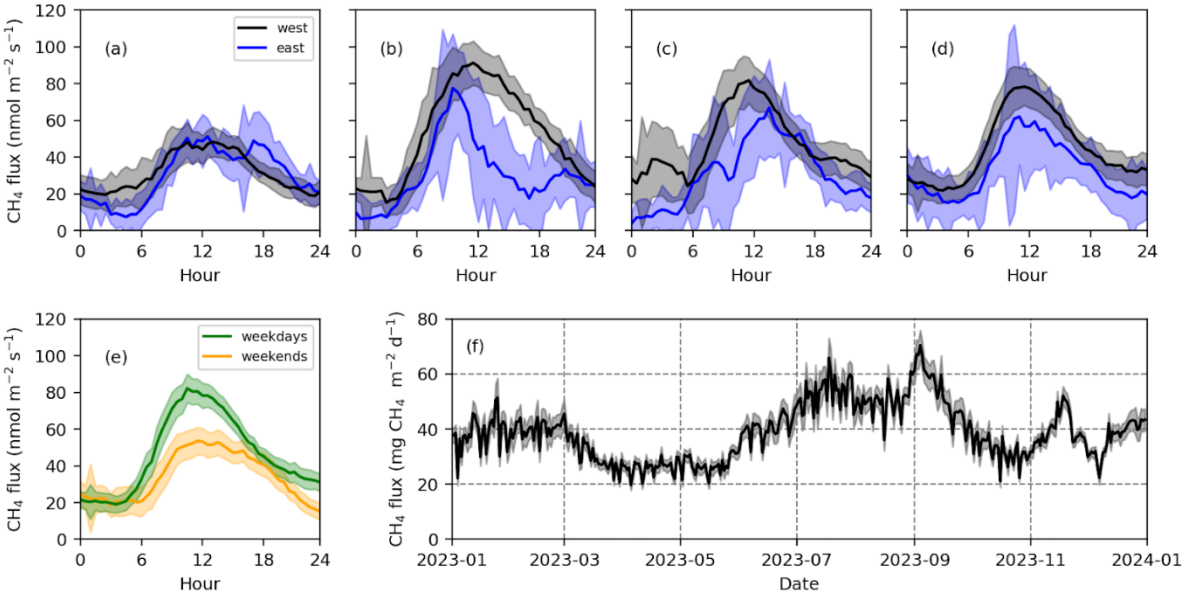

https://doi.org/10.5194/egusphere-2024-3926
Preprint. Discussion started: 3 February 2025

Fig. 10. CH_4 fluxes measured via the eddy covariance method in 2023. Mean diurnal variation in CH_4 fluxes from March to May (a), from June to August (b), from September to November (c), from December to February (d), and for the whole year for weekdays and weekends (e). The black symbols in (a–d) represent the fluxes for the western sector, and the blue symbols represent the eastern sector. The shading in (a–e) indicates the standard error of the measured CH_4 fluxes at each time point. The daily CH_4 flux for 2023, where the shading represents the standard error based on 100 bootstrap samples in gap filling (f).

4. Discussion

The annual CH_4 emissions in Osaka (10,021 ± 1,000 $tCH_4\ yr^{-1}$) and Sakai (2,379 ± 480 $tCH_4\ yr^{-1}$) according to the vehicle measurements were considerably higher than those reported by the local government: 560 $tCH_4\ yr^{-1}$ for Osaka city in 2021 (https://www.city.osaka.lg.jp/kankyo/cmsfiles/contents/0000352/352849/2022jimujigyouhen(1--5).pdf) and 960 $tCH_4\ yr^{-1}$ for Sakai city (https://www.city.sakai.lg.jp/kurashi/gomi/ondanka/oshirase/GHGemissions2020.files/sakai2020_ghg3.pdf) in 2017. Our estimates of CH_4 emissions were 18 times greater for Osaka and 2.5 times greater for Sakai than for the above emission reports. According to reports from local governments, CH_4 emissions from wastewater treatment account for 98% of the total CH_4 emissions in Osaka city and 86% of the total CH_4 emissions in Sakai city. The current measurements indicate that potentially unaccounted biological sources (sewer pipes, plants for fermented foods, reservoirs, ditches of ancient tombs, river sides, dairy farms, and composts) were also present in addition to wastewater treatment plants. The measurements also revealed that natural gas-related sources accounted for 64% of the total in Osaka city and 47% of the total in Sakai city (75% according to the bicycle measurements). CH_4 emissions from these natural gas sources are currently not accounted for in the reports of the local government, resulting in considerable underestimates of CH_4 emissions.

The estimated natural gas CH_4 emissions (6,389 ± 520 $tCH_4\ yr^{-1}$ in Osaka and 1,188 ± 433 $tCH_4\ yr^{-1}$ for Sakai) were comparable to or even higher than those reported for European and North American countries. Vogel et al. (2024) reported that CH_4 emissions in 12 cities ranged from 50–5,000 $tCH_4\ yr^{-1}$, roughly corresponding to fluxes of 1–8 $tCH_4\ km^{-2}\ yr^{-1}$. The natural gas emissions for Osaka city (28 ± 2 $tCH_4\ km^{-2}\ yr^{-1}$) were greater than this range, and those for Sakai city (8 ± 3 $tCH_4\ km^{-2}\ yr^{-1}$) were in the middle to high range. Compared with previous studies in European and North American countries, the emission characteristics were different. The CH_4 LIs for Osaka and Sakai were mostly characterized by low enhancements, but the density of LIs was much greater than that reported in previous studies. This result indicated that a number of small CH_4 sources contributed to the total fluxes, whereas no large emission sources were found in our measurements. Vogel et al. (2024) reported that the top 10% of emissions accounted for 60–80% of the total emissions in European and North American countries, which contrasts with our results in Japan. Notably, without the calibration using the EC measurements (i.e., when A = 1.0 was applied in Eq. 5), the natural gas CH_4 emissions (158 to 3,395 $tCH_4\ yr^{-1}$ in Osaka and 25 to 465 $tCH_4\ yr^{-1}$ for Sakai, where ranges are based on 4 different empirical equations) were similar to those for the European and North American cities, where previous studies did not apply this correction. We discuss the uncertainties associated with this

https://doi.org/10.5194/egusphere-2024-3926
Preprint. Discussion started: 3 February 2025

correction later. Even without the calibration, the natural gas emissions in Osaka city according to the mobile measurements ranged from 25% according to Eq. 7 to 606% according to Eq. 9 of the total CH_4 emissions from Osaka city according to the inventory and were far greater than the inventory-based CH_4 emissions subtracted by the contribution of sewage (12 tCH_4 yr^{-1}).

The current measurements indicate that restaurants are an important CH_4 source co-emitting C_2H_6. One possibility for the emissions was the use of cast iron stoves for cooking in restaurants, where there may be unintentional gas leakage during on/off pulses (Lebel et al., 2022) because stoves that use natural gas are lit manually. Current duplicated measurements in a market street revealed that LIs were detected during the daytime but not during the early morning hours before restaurants were open. These results suggest that LIs from restaurants are not associated with steady gas leakage from pipelines but are related to intermittent leakage during gas use. The results further suggest that introducing built-in electronic ignition could reduce CH_4 emissions from restaurants in Japan. Label et al. (2022) reported that stoves using pilot lights resulted in considerably high CH_4 emissions for residential homes in the USA. CH_4 emissions from restaurants were not previously reported via mobile measurements in USA and European cities. The detection of CH_4 emissions near restaurants could be partly associated with narrow streets in Japanese cities. In the current vehicle measurements, the distance between the air inlet and restaurants near roads is approximately 2 m on narrow streets, 4 m on 1 lane roads on each side, and 5–9 m on the main roads. The close distance between the air inlet and restaurants could contribute to the effective detection of CH_4 enhancements.

The EC measurements revealed that CH_4 emissions underwent a clear diurnal variation (Fig. 10), where nighttime emissions were low, but emissions increased during the day. These results indicate that estimating CH_4 emissions via daytime mobile measurements might be overestimated if diurnal variations in LIs are not accounted for. On the basis of EC measurements (Gioli et al., 2013; Helfer et al., 2016; Huangfu et al., 2024; Pawlak and Fortuniak, 2016), similar diurnal variations were also observed in European and Chinese cities, although the ranges in the diurnal variations were greater in Sakai than in other cities (Huangfu et al., 2024). The nighttime emissions in Sakai were comparable to those measured in Łódź (20–25 nmol m^{-2} s^{-1}) but lower than those measured in other cities (100 nmol m^{-2} s^{-1}) in London (Helfer et al., 2016), Florence (Gioli et al., 2013), and Beijing (Huangfu et al., 2024). A small nighttime CH_4 flux could suggest that steady gas leaks are small in Sakai because CH_4 emissions would be high at night if steady gas leaks were more important. The daytime increase in CH_4 fluxes could be associated with increased human activities. The daytime fluxes were greater than those in Łódź (30–35 nmol m^{-2} s^{-1}) but lower than those in London (150–200 nmol m^{-2} s^{-1}), Florence (170 nmol m^{-2} s^{-1}), and Beijing (200 nmol m^{-2} s^{-1}).

A comparison of CH_4 emissions between Osaka and Sakai indicated that urban intensity increased CH_4 emissions and decreased contributions to biogenic emissions. The biogenic and natural gas CH_4 emissions in Osaka city were more than 2.8 and 3.8 times higher than those in Sakai city, respectively. Human activities, such as the use of natural gas and sewage water,

https://doi.org/10.5194/egusphere-2024-3926
Preprint. Discussion started: 3 February 2025

could cause high emissions in highly urbanized cities, such as Osaka city. The use of natural gas in Osaka city is 3.4 times greater than that in Sakai city. The number of sewage plants visited in Osaka city was 1.8 times greater than that visited in Sakai city in terms of treatment capacity. These gradients of urban intensity could explain the differences in CH_4 emissions among cities in Japan. Measurements in rural areas in Sakai (i.e., Minami Ward in Sakai city) indicated that biological sources, such as dairy farms, composts and reservoirs, played an important role in regional CH_4 emissions. This suggests that biological CH_4 emissions could be important in rural areas in Japan.

A comparison of the vehicle and bicycle measurements revealed that the total CH_4 emissions did not differ substantially. This result indicates that vehicle measurements, albeit with limited coverage, are useful for estimating urban CH_4 emissions in Japan. In contrast, the source attributions differed between the two measurements. This inconsistency could be explained by the research design. We prioritized visiting known biogenic sources, such as sewage plants, in the vehicle measurements, resulting in high bias in biogenic sources. For the natural gas CH_4 LIs, the LI densities were greater in the vehicle measurements (0.19 km^{-1}) than in the bicycle measurements (0.12 km^{-1}) for the same area (Kita, Sakai, and Naka Wards). These results indicate that greater natural gas CH_4 emissions occurred in streets accessible to vehicles with higher levels of human activity, and biases for not covering narrow streets did not cause underestimates for natural gas LIs.

We stress that mobile measurements could underestimate CH_4 emissions from sewage plants because the detected CH_4 enhancements were generally small (Fig. A4). The current study did not intend to improve estimates of large point sources that were already accounted for in the local government reports but rather aimed to identify the missing sources. The underestimates could be associated with the distance to emission sources in a sewage plant (e.g., sedimentation pond and exposure tanks) from public roads where the measurements were made. CH_4 can be emitted at high altitudes (e.g., smokestacks), and these emissions may not be detected by mobile measurements on the ground. CH_4 emissions measured via the EC method were found to be greater when the flux footprint consisted of sewage plants in Sakai (Takano and Ueyama, 2021). These results indicate that sewage plants are important CH_4 sources, as accounted for in the reporting of the local government. Consequently, the CH_4 emissions in the current study were considerably underestimated or even did not account for these sources. Repeated measurements around point sources could improve the accounting of CH_4 emissions for point sources by inversely applying plume models (Stadler et al., 2022). The high C_2:C_1 ratios measured near the sewage plants might indicate the occurrence of combustion processes in the sewage plants.

Simultaneous measurements of the two different inlet heights of the vehicle revealed that a low measurement height effectively detected LIs. These findings suggest that lower measurement heights are suitable for detecting urban CH_4 emissions in Japanese cities. In previous studies that conducted mobile measurements (Vogel et al., 2024), inlets were mostly installed at the front bumper or top of the roof, where the inlet heights were, for example, 0.5 m (Maazallahi et al., 2020), 0.6 m (Fernandez et al., 2022), 1.3 m (Takano & Ueyama, 2021), 2 m for bicycles and 2.5 m for vehicles (Ars et al.,

https://doi.org/10.5194/egusphere-2024-3926
Preprint. Discussion started: 3 February 2025

2020), and 3 m (Phillips et al., 2013). The effective height could differ in each city depending on the emission strength and major source type. This highlights the need for consistent methodologies across study teams conducting this type of work, or at the very least, the development of transfer functions between instruments and mounting positions. A better understanding of the effective inlet height in a target city or country would improve estimates of urban CH_4 emissions.

Simultaneous measurements of CH_4 and C_2H_6 concentrations enabled us to understand the source attributions of CH_4 emissions. Two clear clusters in the C_2:C_1 ratio separating biological and natural gas sources were observed in the current mobile measurements (Fig. 3), where the C_2:C_1 ratios for natural gas sources almost coincided with those for natural gas by the local gas company. This result suggests that the measurements sufficiently captured the emission plume before it became substantially diluted, although the slope was a somewhat smaller C_2:C_1 ratio than those distributed by the local gas company. Previously, source attributions were determined via simultaneous measurements of C_2H_6 concentrations (Fernandez et al., 2022; Hopkins et al., 2016; Maazallahi et al., 2020) and the isotopic composition of CH_4 (Fernandez et al., 2022; Defrathyka et al., 2021; Maazallahi et al., 2020; Phillips et al., 2013).

In this study, upscaled fluxes and areal emissions were calibrated with CH_4 fluxes measured via the EC method in terms of daytime CH_4 fluxes and diurnal variations in fluxes. This calibration was necessary because empirical models (Weller et al., 2019; Weitzel and Schmidt, 2023; Joo et al., 2024; Umezawa et al., in preparation) underestimate the CH_4 flux measured via the EC method. The discrepancies in the empirical models in the Osaka metropolitan area might be explained by different emission characteristics between Osaka and the corresponding control experiments. Because the LIs of cities in the USA and European cities are related mostly to gas leaks from underground pipelines, control experiments for developing empirical equations have been designed to effectively capture CH_4 emissions from roads directly beneath them (Weller et al., 2019; Weitzel and Schmidt, 2023; Joo et al., 2024). In contrast, LIs for Osaka could be related to small sources, such as restaurants (LIs from sides, such as doors and ventilation fans), farmlands, manholes or reservoirs (no gas-diffusion resistance in the soil). For such LIs, CH_4 enhancement could be underestimated because overground emission plumes could be advected both horizontally and vertically, resulting in underestimates of CH_4 emission by roadside measurements with the empirical model. The control experiment by Uemezawa et al. (in preparation) was designed to characterize plume CH_4 emissions, where CH_4 was emitted from a 5-m-high pipe and was measured at a horizontal distance of approximately 50 m. Interestingly, among the four empirical models, the *A* factor for their equation was the smallest, meaning that the underestimates for Japanese cities were minimized among the available empirical models. These results suggest that emissions in the Osaka metropolitan area are largely associated with horizontal plumes. Similar underestimates in the use of Weller's empirical model were reported with mobile measurements in Toronto, Canada (Ars et al., 2020). Compared with other empirical models (von Fischer et al., 2017), the Weller model was a third lower than the CH_4 emissions estimated in Toronto, owing to the Weller model not accounting for low emissions. It is therefore inferred that synthesis analyses for different cities with a single empirical model involve unaccounted uncertainty that has not been examined (Vogel et al. 2024). The calibration could also

https://doi.org/10.5194/egusphere-2024-3926
Preprint. Discussion started: 3 February 2025

cause uncertainties because the calibration was the major daytime footprint of the EC method and was applied to other areas. This could cause artifacts if the emission characteristics differ between the calibrated area (i.e., Sakai Ward) and other areas (e.g., Osaka city). Although the calibration induces uncertainties, there are 21 uncertainties in the regional fluxes according to the uncalibrated empirical models. Further EC measurements at multiple locations could help reduce artifacts and develop further practical calibration methods.

The discrepancy between the EC results and mobile measurements could also be caused by potential CH_4 sources that were not well detected by the mobile measurements. The mismatch between top-down and mobile measurements has also been reported in another city, namely, Hamburg, Germany (Forstmaier et al., 2023), where approximately 10 times greater CH_4 emissions were estimated via the top-down method than via mobile measurements. They argued that undetected source emissions by mobile measurements could cause large discrepancies, which include CH_4 emitted from stoves in residential homes (Lebel et al., 2022) and residential gas meter assemblies (Vollrath et al., 2024). In Sakai, we used direct measurements to record a 3.7 ppm CH_4 concentration in the exhaust of a gas-generated air conditioner installed at the roof of a building at Osaka Metropolitan University. If such sources (e.g., not located near the ground) are important in Osaka and Sakai, the upscaling of CH_4 emissions by the calibrated mobile measurements contains considerable uncertainties, irrespective of the consistency with the EC measurements.

In addition to the calibration by the EC measurements, we mention potential limitations and improvements for the mobile measurements. In this study, we prioritized broader and higher-density measurements over reproducibility, primarily focusing on the urban landscape. This research design was poor at distinguishing steady LIs from LIs that randomly occur because previous studies suggest that 5–8 repeated measurements improved the frequency, enhancement, and magnitude of CH_4 leaks (Luetschwager et al., 2021). Because mobile measurements were conducted during the fallow season, CH_4 emissions from rice paddies were not accounted for in this study. Seasonal and daily variations in the biological sources, including wastewater treatment, were also not captured with the current intensive measurements. Biological sources from reservoirs and ditches could also be greater in summer than in other seasons; thus, biological fluxes could be greater than those currently estimated in this study. In contrast, we planned visiting sewage facilities as a research design, which might overestimate the frequency of detecting LIs associated with biological sources. This might explain why the vehicle measurements detected more biological CH_4 emissions than did the bicycle measurements (Fig. 7). Potentially large CH_4 sources, such as farmlands and sedimentation ponds in sewage plants, are located to some degree distant from public roads. The measured CH_4 enhancements might be biased toward only smaller nearby sources that result in sharp peaks, resulting in the underestimation of CH_4 emissions from larger, more diffuse sources. Obtaining measurement permission in private areas, such as industrial sites, could also help better characterize high-emission categories. Finally, we assumed that the current mobile measurements were also representative of the areal characteristics of CH_4 emissions from city areas that were not measured in this study. Because this study included dense urban centers in Osaka city down to rural areas in Sakai city, the

https://doi.org/10.5194/egusphere-2024-3926
Preprint. Discussion started: 3 February 2025

measurements covered most major land uses in Osaka Prefecture and should represent the emission characteristics in Osaka. This assumption and potential limitations will be validated with future measurements that include areas that were not measured in this study.

5. Conclusions

We conducted two measurement campaigns involving mobile measurements and EC measurements in the Osaka metropolitan area from 2023–2024. The measurements indicated that Osaka and Sakai were the sources of CH_4, and the CH_4 emissions from natural gas contributed 44 to 74%. The magnitude of emissions was comparable to those reported in cities in Europe and North America. However, the estimates would become smaller CH_4 emissions than those for the other cities if the same upscaling methodology used in many other studies was used. We found various types of LIs in the cities, which were not accounted for in the current inventories of the local government. These unaccounted sources should be well characterized with inventory systems and could be considered for mitigating climate change. Further mobile measurements for areas currently not measured and other cities in Japan and long-term EC measurements will allow better characterization of CH_4 emissions in Japan. The estimates of CH_4 emissions via mobile measurements currently have considerable uncertainties, and we calibrated the upscaled fluxes with the EC measurements. Future studies should revisit improvements in empirical estimation methods based on other top-down methods, such as atmospheric or EC measurements. Further understanding the reasons for the discrepancy between the top-down EC measurements and mobile measurements is key to understanding the mitigation potential for urban methane in Japan.

Competing interests

The authors declare that they have no conflict of interest.

Acknowledgments

This study was supported by the Environmental Defense Fund and JSPS KAKENHI, grant number 24K03065. The vehicle measurements were supported by CLIMATEC, Inc., especially Yoshiyuki Yanagawase and Toshiki Sugiyama. The bicycle measurements were supported by Yuriko Ueyama and Akira Nakaoka of Osaka Metropolitan University. We thank the staff of the Sakai City Office for supporting the measurements. The total road length for each administrative division was provided by Sakai city and Osaka city. Permission was made by Osaka Prefecture to reach the final disposal site at Pier 7-3 in Sakai Ward. Osaka Gas Network Co., Ltd. provided information about local gas distributions and potential emission sources.

https://doi.org/10.5194/egusphere-2024-3926
Preprint. Discussion started: 3 February 2025

References

Ando, T., and Ueyama, M.: Surface energy exchange in a dense urban built-up area based on two-year eddy covariance measurements in Sakai, Japan, Urban Climate, 19, 155-169, https://doi.org/10.1016/j.uclim.2017.01.005, 2017.

Ars, S., Vogel, F., Arrowsmith, C., Heerah, S., Knuckey, E., Lavoie, J., Lee, C., Pak, N. M., Phillips, J. L., and Wunch, D.: Investigation of the spatial distribution of methane sources in the greater Toronto area using mobile gas monitoring systems, Environmental Science & Technology 54, 15671-15679, https://doi.org/10.1021/acs.est.0c05386, 2020.

Baldocchi, D.: Measuring fluxes of trace gases and energy between ecosystems and the atmosphere - the state and future of the eddy covariance method, Global Change Biology, 20, 3600-3609, https://doi.org/10.1111/gcb.12649, 2014.

Commane, R., Hallward-Driemeier, A., and Murray, L. T.: Intercomparison of commercial analyzers for the atmospheric ethane and methane observations, Atmospheric Measurement Technologies, 16, 1431-1441, https://doi.org/10.5194/amt-16-1431-2023, 2023.

Crippa, M., Guizzardi, D., Pisoni, E., Solazzo, E., Guion, A., Muntean, M., Florczyk, A., Schiavina, M., Melchiorri, M., and Hutfilter, A. F.: Global anthropogenic emissions in urban areas: patterns, trends, and challenges, Environmental Research Letters, 16, 074033, https://doi.org/10.1088/1748-9326/ac00e2, 2021.

Defratyka, S. M., Paris, J.-D., Yver-Kwok, C., Fernandez, J. M., Korben, P., and Bousquet, P.: Mapping urban methane sources in Paris, Fance, Environmental Science & Technology, 55, 8583-8591, https://doi.org/10.1021/acs.est.1c00859, 2021.

Gioli, B., Toscano, P., Zaldei, A., Fratini, G., and Miglietta, F.: CO_2, CH_4 and particles flux measurements in Florence, Italy, Energy Procedia, 40, 537-544, https://doi.org/10.1016/j.egypro.2013.08.062, 2013.

Falge, E., et al.: Gap filling strategies for defensible annual sums of net ecosystem exchange, Agricultural and Forest Meteorology, 107, 43-69, https://doi.org/10.1016/S0168-1923(00)00225-2, 2001.

Fernandez, J. M., Maazallahi H., France, J. L., Menoud, M., Corbu, M., Ardelean, M., Calcan, A., Townsend-Small, A., van der Veen, C., Fisher, R. E., Lowry, D., and Nisbet, E. G.: Street-level methane emissions of Bucharest, Romania and the dominance of urban wastewater, Atmospheric Environment X, 13, 100153, https://doi.org/10.1016/j.aeaoa.2022.100153, 2022.

Forstmaier, A., Chen, J., Dietrich, F., Bettinelli, J., Maazallahi, H., Schneider, C., Winkler, D., Zhao, X., Jones, T., van der Veen, C., Wildmann, N., Makowski, M., Uzun, A., Klappenbach, F., van der Gon, H. D., Scwietzke, S., and Röchmann, T.: Quantification of methane emissions in Hamburg using a network of FTIR spectrometers and an inverse modelling approach, Atmospheric Chemistry and Physics 23, 6897–6922, https://doi.org/10.5194/acp-23-6897-2023, 2023.

Helfter, C., Tremper, A. H., Halios, C. H., Kotthaus, S., Bjorkegren, A., Grimmond, C. S. B., Barlow, J. F., and Nemitz, E.: Spatial and temporal variability of urban fluxes of methane, carbon monoxide and carbon dioxide above London, UK, Atmospheric Chemistry and Physics, 16, 10543–10557, https://doi.org/10.5194/acp-16-10543-2016, 2016.

https://doi.org/10.5194/egusphere-2024-3926
Preprint. Discussion started: 3 February 2025

Huangfu, Y., Yuan, B., He, X., Liu, Z., Zhang, Y., Karl, T., Striednig, M., Ding, Y., Chen, X., Li, H., Zheng, H., Chang, M., Wang, X., and Shao, M.: Natural gas leakage ratio determined from flux measurements of methane in urban Beijing, Environmental Science & Technology Letters, 11, 1025-1031, https://doi.org/10.1021/acs.estlett.4c00573, 2024.

Hopkins, F. M., Kort, E. A., Bush, S. E., Ehleringer, J. R., Lai, C.-T., Black, D. R., and Randerson, J. T.: Spatial patterns and source attribution of urban methane in the Los Angels Basin, Journal of Geophysical Research Atmosphere, 121, 2490-2507, https://doi.org/10.1002/2015JD024429, 2016.

Ito, A., Tohjima, Y., Saito, T., Umezawa, T., Hajima, T., Hirata, R., Saito, M., and Terao, Y.: Methane budget of East Asia, 1990-2015: A bottom-up evaluation, Science of the Total Environment, 676, 40-52, https://doi.org/10.1016/j.scitotenv.2019.04.263, 2019.

Itoh, M., Sudo, S., Mori, S., Saito, H., Yoshida, T., Shiratori, Y., Suga, S., Yoshikawa, N., Suzue, Y., Mizukami, H., Mochida, T., and Yagi, K.: Mitigation of methane emissions from paddy fields by prolonging midseason drainage, Agriculture, Ecosystems and Environment, 141, 359-372, https://doi.org/10.1016/j.agee.2011.03.019, 2011.

Jackson, R. B., Down, A., Phillips, N. G., Ackley, R. C., Cook, C. W., Plata, D. L., and Zhao, K.: Natural gas pipeline leaks across Washington, DC, Environmental Science and Technology, 48, 2051–2058, https://doi.org/10.1021/es404474x, 2014.

Joo, J., Jeong, S., Shin, J., and Chang, D. Y.: Missing methane emissions from urban sewer networks, Environmental Pollution, 342, 123101, https://doi.org/10.1016/j.envpol.2023.123101, 2024.

Lebel, E. D., Finnegan, C. J., Ouyang, Z., and Jackson, R. B.: Methane and NO_x emissions from natural gas stoves, cooktops, and ovens in residential homes, Environmental Science and Technology, 56, 2529–2539, https://doi.org/10.1021/acs.est.1c04707, 2022.

Liu, Z., Liu, Z., Song, T., Gao, W., Wang, Y., Wang, L., Hu, B., Xin, J., and Wang, Y.: Long-term variation in CO_2 emissions with implications for the interannual trend in $PM_{2.5}$ over the last decade in Beijing, China, Environmental Pollution, 266, 115014, https://doi.org/10.1016/j.envpol.2020.115014, 2020.

Luetschwager, E., von Fischer, J. C., and Weller, Z. D.: Characterizing detection probabilities of advanced mobile leak surveys: implications for sampling effort and leak size estimation in natural gas distribution systems, Elements Science of the Anthropocene, 9, 1, https://doi.org/10.1525/elementa.2020.00143, 2021.

Maazallahi, H., Fernandez, J. M., Menoud, M., Zavala-Ariza, D., Welker, Z. D., Schwietzka, S., von Fischer, J. C., van der Gon, H. D., and Röckmann, T.: Methane mapping, emission quantification, and attribution in two European cities: Utrecht (NL) and Hamburg (DE), Atmospheric Chemistry and Physics, 20, 14717–14740, https://doi.org/10.5194/acp-20-14717-2020, 2020.

McDermitt, D., Burba, G., Xu, L., Anderson, T., Komissarov, A., Riensche, B., Schedlbauer, Starr G., Zona, D., Oechel, W., Oberbauer, S., and Hastings, S.: A new low-power, open-path instrument for measuring methane flux by eddy covariance. Applied Physics B Lasers Optics, 102, 391–405, https://doi.org/10.1007/s00340-010-4307-0, 2011.

https://doi.org/10.5194/egusphere-2024-3926
Preprint. Discussion started: 3 February 2025

National Greenhouse Gas Inventory Document of JAPAN 2024 (NGGIDJ, 2024): In: Greenhouse Gas Inventory Office of Japan and Ministry of the Environment, Japan (Ed.), Center for Global Environmental Research, Earth System Division, National Institute for Environmental Studies, Japan, 794 pp, https://www.env.go. jp/, 2024.

Moore, C.J.: Frequency response corrections for eddy correlation systems, Boundary-Layer Meteorology, 37, 17–35, https://doi.org/10.1007/BF00122754, 1986.

Nordbo, A., Järvi, L., Haapanala, S., Wood, C. R., and Vesala, T.: Fraction of natural area as main predictor of net CO_2 emissions from cities, Geophysical Research Letters, 39, L20802, https://doi.org/10.1029/2012GL053087, 2012.

Okamura, S., Ueyama, M., and Takahashi, K.: Temporal and spatial variations in NO_2 fluxes by tall tower eddy covariance measurements over a dense urban center in Sakai, Japan. Atmospheric Environment, 339, 120870, https://doi.org/10.1016/j.atmosenv.2024.120870, 2024.

Pawlak, W., and Fortuniak, K.: Eddy covariance measurements of the net turbulent methane flux in the city center - results of 2-year campaign in Łódź, Poland, Atmospheric Chemistry and Physics, 16, 8281–8294, https://doi.org/10.5194/acp-16-8281-2016, 2016.

Phillips, N. G., Ackley, R., Crosson, E. R., Down, A., Hutyra, L. R., Brondfield, M., Karr, J. D., Zhao, K., and Jackson, R. B.: Mapping urban pipeline leaks: methane leaks across Boston, Environmental Pollution, 173, 1-4, https://doi.org/10.1016/j.envpol.2012.11.003, 2013.

Sargent M. R., Floerchinger, C., McKain K., Budney, J., Gottlieb, E. W., Hutyra, L. R., Rudek, J., and Wofsy, S. C.: Majority of US urban natural gas emissions unaccounted for in inventories, Proceedings of National Academy of Science U.S.A., 118(44), e2105804118, https://doi.org/10.1073/pnas.2105804118, 2021.

Stadler, C., Fusé, V. S., Linares, S., and Juliarena, P.: Estimation of methane emission from an urban wastewater treatment plant applying inverse Gaussian model, Environmental Monitoring and Assessment, 194, 27, https://doi.org/10.1007/s10661-021-09660-4, 2022.

Takano, T., and Ueyama, M.: Spatial variations in daytime methane and carbon dioxide emissions in two urban landscapes, Sakai, Japan, Urban Climate, 36, 100798, https://doi.org/10.1016/j.uclim.2021.100798, 2021.

Ueyama, M., and Ando, T.: Diurnal, weekly, seasonal, and spatial variabilities in carbon dioxide flux in different urban landscapes in Sakai, Japan, Atmospheric Chemistry and Physics, 16, 14727–14740, https://doi.org/10.5194/acp-16-14727-2016, 2016.

Ueyama, M., Hirata, R., Mano, M., Hamotani, K., Harazono, Y., Hirano, T., Miyata, A., Takagi, K., and Takahashi, Y.: Influences of various calculation options on heat, water, and carbon fluxes determined by open- and closed-path eddy covariance method, Tellus B, 64, 19048, https://doi.org/10.3402/tellusb.v64i0.19048, 2012.

Ueyama, M., Taguchi, A., and Takano, T.: Water vapor emissions from urban landscapes in Sakai, Japan, Journal of Hydrology, 598, 126384, https://doi.org/10.1016/j.jhydrol.2021.126384, 2021.

https://doi.org/10.5194/egusphere-2024-3926
Preprint. Discussion started: 3 February 2025

Ueyama, M., and Takano, T.: A decade of CO_2 flux measured by the eddy covariance method including the COVID-19 pandemic period in an urban center in Sakai, Japan, Environmental Pollution, 304, 119210, https://doi.org/10.1016/j.envpol.2022.119210, 2022.

Umezawa, T., Terao, Y., Ueyama, M., Lunt, M., and France, J. L.: Mobile measurements to estimate urban methane emissions in Tokyo, In preparation for submitting to Atmospheric Chemistry and Physics.

Vickers, D., and Mahrt, L.: Quality control and flux sampling problems for tower and aircraft data, Journal of Atmospheric and Oceanic Technology, 14, 512–526, https://doi.org/10.1175/1520-0426(1997)014<0512:QCAFSP>2.0.CO;2, 1997.

Vogel, F., Ars, S., Wunch, D., Lavoie, J., Gillespie, L., Maazallahi, Röckmann, T., Nęcki, J., Bartyzel, J., Jagoda, P., Lowry, D., France, J., Fernandez, J., Bakkaloglu, S., Fisher, R., Lanoiselle, M., Chen, H., Oudshoorn, M., Yver-Kwok, C., Defratyka, S., Morgui, J. A., Estruch, C., Curcoll, R., Grossi, C., Chen, J., Dietrich, F., Forstmaier, A., Denier van der Gon, H. A. C., Dellaert, S. N. C., Salo, J., Corbu, M., Iancu, S. S., Tudor, A. S., Scarlat, A. I., and Calcan, A.: Ground-Based Mobile Measurements to Track Urban Methane Emissions from Natural Gas in 12 Cities across Eight Countries. Environmental Science & Technology, 58, 2271-2281, https://pubs.acs.org/doi/10.1021/acs.est.3c03160, 2024.

Vollrath, C., Hugenholtz, C. H., Barchyn, T. E., and Wearmouth, C.: Methane emissions from residential natural gas meter set assemblies, Science of the Total Environment, 931, 172857, https://doi.org/10.1016/j.scitotenv.2024.172857, 2024.

von Fischer, J. C., Cooley D., Chamberlain, S., Gaylord, A., Griebenow, C. J., Hamburg, S. P., Salo, J., Schumacher, R., Theobald, D., and Ham, J.: Rapid, vehicle-based identification of location and magnitude of urban natural gas pipeline leaks, Environmental Science & Technology, 51, 4091-4039, https://doi.org/10.1021/acs.est.6b06095, 2017.

Webb, E.K., Pearman, G.I., and Leuning, R.: Correction of flux measurements for density effects due to heat and water vapour transfer, Quarterly Journal of the Royal Meteorological Society, 106, 85–100, https://doi.org/10.1002/qj.49710644707, 1980.

Weller, Z. D., Yang, D. K., and von Fischer, J. C.: An open source algorithm to detect natural gas leaks from mobile methane survey data, PLoS ONE, 14, e0212287, https://doi.org/10.1371/journal.pone.0212287, 2019.

Wietzel, J. B., and Schmidt, M.: Methane emission mapping and quantification in two medium-sized cities in Germany: Heidelberg and Schwetzingen, Atmospheric Environment X, 20, 100228, https://doi.org/10.1016/j.aeaoa.2023.100228, 2023.

https://doi.org/10.5194/egusphere-2024-3926
Preprint. Discussion started: 3 February 2025

Appendix

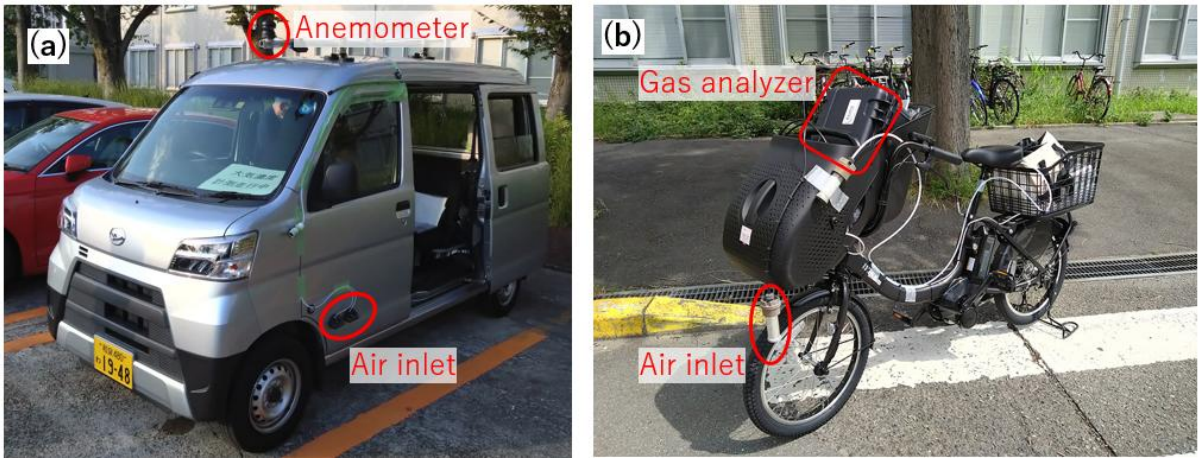

Figure A1. Mobile measurement system using a vehicle (a) and bicycle (b).

https://doi.org/10.5194/egusphere-2024-3926
Preprint. Discussion started: 3 February 2025

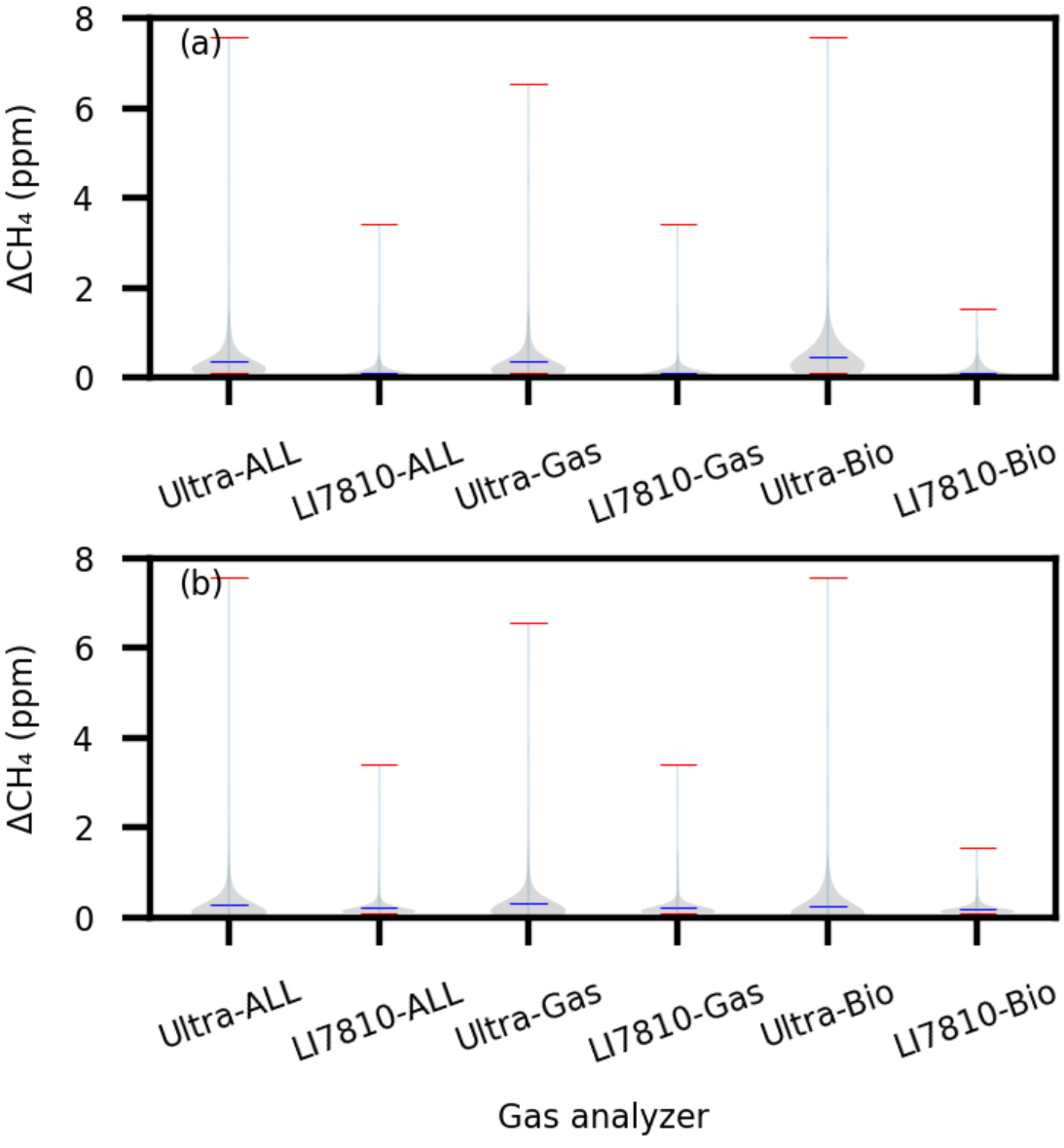

Figure A2. Violin plots for ΔCH_4 enhancements (ΔCH_4) measured at LIs based on the vehicle measurements by the Mira Ultra analyzer installed at 0.5 m above the ground and the LI-7810 analyzer at 1.85 m. The plots are summarized for natural gas and biological sources as well as for all LIs. The source attributions are based on C_2:C_1 for the Ultra analyzer and ΔCH_4 for the LI-7810 analyzer. Subplot (a) is ΔCH_4 identified by the Ultra analyzer, and (b) is ΔCH_4 identified by the LI-7810 analyzer.

https://doi.org/10.5194/egusphere-2024-3926
Preprint. Discussion started: 3 February 2025

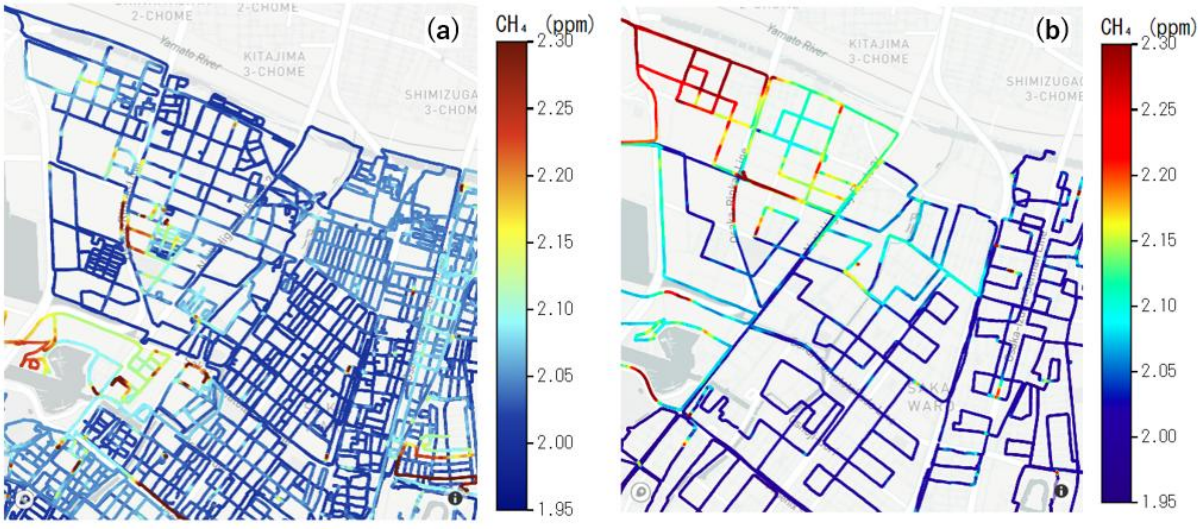

Figure A3. CH_4 concentrations based on the bicycle (a) and vehicle (b) measurements for Sakai Ward as an example of how intensively the bicycle measurements covered the streets compared with the vehicle measurements. To remove the daily variations in the CH_4 concentration for visualization, the CH_4 concentration was rescaled so that the 5th percentile of the CH_4 concentration on each measurement day was 2.0 ppm. Visualisation was achieved by the ploty in python which uses OpenStreetMap© as a basemap provided by mapbox©.

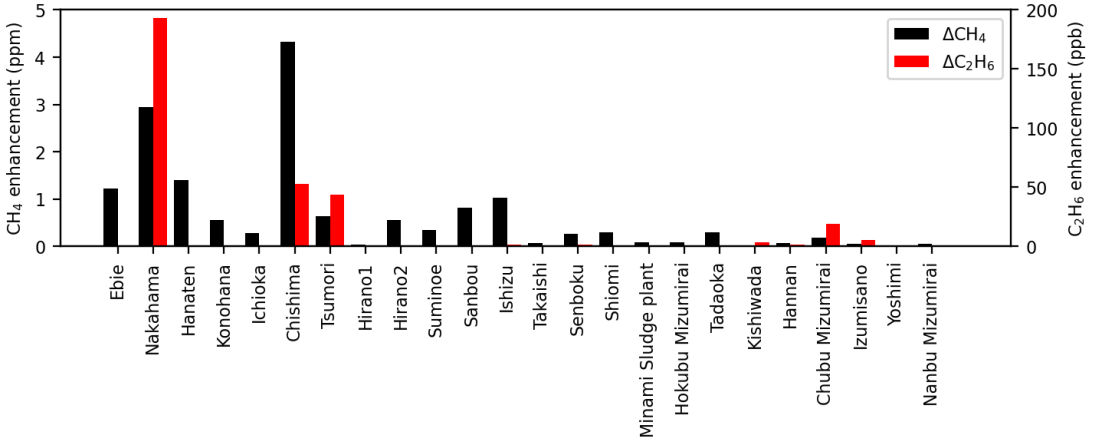

Figure A4. CH_4 and C_2H_6 enhancements within 500 m of a sewage plant based on vehicle measurements. Note that the Minami sludge plant was the only sludge plant, and the others were sewage plants or pump stations. The enhancements could be slightly biased, especially when the wind directions were not ideal, because the concentrations were measured on public roads, which hampered driving circles around all the sewage plants.

https://doi.org/10.5194/egusphere-2024-3926
Preprint. Discussion started: 3 February 2025

860

Table A1. Date, travel distance, speed, and the type of the gas analyzer used in the campaign for the vehicle measurements.

Date	Driving distance (km)	Speed (km hr^{-1})	Ananlyzer	Date	Driving distance (km)	Speed (km hr^{-1})	Ananlyzer
2023/5/18	107.9	23.9	Ultra	2023/11/17	81.5	13.1	Ultra / LI-7810
2023/9/25	57.4	23.1	Ultra / LI-7810	2023/11/21	52.1	43.4	Ultra
2023/9/26	95.9	16.5	Ultra / LI-7810	2023/11/21	54.1	36.9	Ultra
2023/9/27	78.2	12.9	Ultra / LI-7810	2023/11/22	52.0	19.7	Ultra
2023/9/28	78.7	12.3	Ultra / LI-7810	2023/11/25	112.4	23.0	Ultra
2023/9/29	52.2	12.1	Ultra / LI-7810	2023/12/11	77.3	12.5	Ultra / LI-7810
2023/10/9	81.1	19.4	Ultra / LI-7810	2023/12/12	119.7	17.2	Ultra / LI-7810
2023/10/10	89.5	12.7	Ultra / LI-7810	2023/12/13	144.1	17.5	Ultra / LI-7810
2023/10/11	72.3	11.2	Ultra / LI-7810	2023/12/14	122.1	18.3	Ultra / LI-7810
2023/10/12	86.0	11.7	Ultra / LI-7810	2023/12/15	89.4	14.4	Ultra / LI-7810
2023/10/13	67.3	11.0	Ultra / LI-7810	2024/11/18	80.9	10.9	Ultra / LI-7810
2023/11/13	119.5	19.2	Ultra / LI-7810	2024/11/19	106.6	14.0	Ultra / LI-7810
2023/11/14	95.1	13.9	Ultra / LI-7810	2024/11/20	95.5	12.1	Ultra / LI-7810
2023/11/15	107.1	14.5	Ultra / LI-7810	2024/11/21	78.4	11.2	Ultra / LI-7810
2023/11/16	103.3	14.1	Ultra / LI-7810				

865

Table A2. Date, travel distance, and speed for the bicycle measurements.

Date	Cycle distance (km)	Speed (km hr^{-1})	Date	Cycle distance (km)	Speed (km hr^{-1})	Date	Cycle distance (km)	Speed (km hr^{-1})
2023/5/26	4.5	13.5	2023/10/31	45.3	8.9	2023/11/20	1.1	1.8
2023/6/7	3.7	10.8	2023/11/1	47.1	8.9	2023/12/10	71.2	11.6
2023/6/7	16.3	10.8	2023/11/2	44.6	9.3	2024/2/20	20.5	9.5
2023/10/19	42.0	8.4	2023/11/3	86.6	11.6	2024/2/20	24.2	8.9
2023/10/21	69.2	12.2	2023/11/7	42.1	9.3	2024/4/19	32.5	10.4
2023/10/22	65.1	11.0	2023/11/8	30.3	9.3	2024/4/26	34.7	10.7
2023/10/24	45.9	9.5	2023/11/9	17.7	7.9	2024/4/29	24.4	10.4
2023/10/26	28.7	9.5	2023/11/13	23.2	10.2	2024/5/4	27.9	10.2
2023/10/28	83.3	11.3	2023/11/15	41.2	9.2	2024/5/10	27.9	11.6
2023/10/29	75.2	10.2	2023/11/16	40.5	9.1			
2023/10/30	27.5	6.7	2023/11/17	17.7	9.3			